Deep-Sea Research II 118 (2015) 73–87

Contents lists available at ScienceDirect

Deep-Sea Research II

journal homepage: www.elsevier.com/locate/dsr2

Aspects of the marine nitrogen cycle of the Chukchi Sea shelf and Canada Basin

Zachary W. Brown [a,*], Karen L. Casciotti [a], Robert S. Pickart [b], James H. Swift [c], Kevin R. Arrigo [a]

[a] Stanford University, 473 Via Ortega, Room 140, Stanford, CA 94305, United States
[b] Woods Hole Oceanographic Institute, Woods Hole, MA, United States
[c] Scripps Institution of Oceanography, La Jolla, CA, United States

ARTICLE INFO

Available online 7 February 2015

Keywords:
Denitrification
Nitrification
Chukchi Sea
Canada Basin
Nitrate
Ammonium

ABSTRACT

As a highly productive, seasonally ice-covered sea with an expansive shallow continental shelf, the Chukchi Sea fuels high rates of sedimentary denitrification. This contributes to its fixed nitrogen (N) deficit relative to phosphorus (P), which is among the largest in the global ocean, making the Chukchi Sea severely N-limited during the phytoplankton growth season. Here, we examine aspects of the N cycle on the Chukchi Sea shelf and the downstream Canada Basin using nutrients, dissolved oxygen (O_2), and the stable isotopes of nitrate (NO_3^-). In the northward flow path across the Chukchi shelf, bottom waters experienced strong O_2 drawdown, from which we calculated a nitrification rate of 1.3 mmol m^{-2} d^{-1}. This nitrification was likely primarily in sediments and directly fueled sedimentary denitrification, historically measured at similar rates. We observed significant accumulations of ammonium (NH_4^+) in bottom waters of the Chukchi shelf (up to $>5\,\mu M$), which were inversely correlated with $\delta^{15}N_{NO_3}$, indicating a sediment source of ^{15}N-enriched NH_4^+. This is consistent with a process of coupled partial nitrification-denitrification (CPND), which imparts significant ^{15}N enrichment and ^{18}O depletion to Pacific-origin NO_3^-. This CPND mechanism is consistent with a significant decrease in $\delta^{18}O_{NO_3}$ relative to Bering Sea source waters, indicating that at least 58% of NO_3^- populating the Pacific halocline was regenerated during its transit across the North Bering and Chukchi shelves, rather than arriving preformed from the Bering Sea slope. This Pacific-origin NO_3^- propagates into the Canada Basin and towards the North Atlantic, being significantly ^{15}N-enriched and ^{18}O-depleted relative to the underlying Atlantic waters.

1. Introduction

The Chukchi Sea is among the most productive regions in the Arctic Ocean (Sakshaug, 2004). It sustains the longest seasonal phytoplankton blooms of any Arctic region (Arrigo and van Dijken, 2011) and attracts significant numbers of migratory seabirds and marine mammals during summer (Loeng et al., 2005). This high productivity is maintained by the primarily northward flow of nutrient-rich water through Bering Strait, which spreads over the expansive Chukchi Sea continental shelf (<200 m depth) and migrates toward the Canada Basin (Codispoti et al., 2005). However, the Chukchi Sea productivity regime is changing rapidly as sea ice is lost from the region. From 1998 to 2009, the open water season has expanded by $\sim$4.5 d yr^{-1}, and proliferation of melt ponds has stimulated massive under-ice blooms, thus allowing phytoplankton net primary production (NPP) to increase substantially (Arrigo and van Dijken, 2011; Brown and Arrigo, 2012; Arrigo et al., 2012).

On this and other shallow and highly productive shelves of the western Arctic Ocean, a large fraction of the organic matter formed in surface waters sinks to the sea floor, fueling not only a productive benthic community but also high rates of sediment denitrification. Chang and Devol (2009) estimate that Arctic shelves contribute 4–13% of the total sink of fixed nitrogen (N) in the global ocean. Due to this significant fixed N loss, NPP on the continental shelves of the western Arctic is widely considered to be N-limited. The Chukchi shelf in particular is among the regions of lowest N* (a measure of the fixed nitrogen excess relative to phosphorus; Gruber and Sarmiento, 1997) in the global ocean (Deutsch and Weber, 2012). In waters with low N*, significant phosphorus (P) remains after N has been exhausted during the growth season. This excess P flows downstream into

* Corresponding author.
E-mail address: zwbrown@alumni.stanford.edu (Z.W. Brown).

http://dx.doi.org/10.1016/j.dsr2.2015.02.009
0967-0645/

the North Atlantic, where it may fuel high rates of N_2-fixation, thus redressing the significant fixed N loss of Arctic shelves (Yamamoto-Kawai et al., 2006).

Given that N is the limiting macronutrient over the Chukchi shelf, it is important to understand the mechanisms of N loss. Because the water column on Arctic shelves is generally well-oxygenated, denitrification, an anoxic microbial process, is restricted to the sediments. The source of nitrate (NO_3^-) that fuels sediment denitrification is a combination of direct NO_3^- flux from the overlying water column and NO_3^- production via nitrification of sediment ammonium (NH_4^+). Horak et al. (2013) recently showed that the latter mechanism of coupled nitrification-denitrification is the most important mechanism of N loss on the Bering Sea shelf. Furthermore, Granger et al. (2011) showed that unlike denitrification fueled by direct NO_3^- flux from the water column, which leaves no isotopic signature (Brandes and Devol, 1997), coupled nitrification-denitrification leads to isotopic enrichment of fixed N in the Bering Sea water column. It is important to determine whether these same N-loss dynamics apply on the Chukchi shelf, and whether this leads to N isotopic enrichment that propagates into the Arctic Ocean downstream.

In addition to the mechanism of N loss, it is equally important to understand the source of fixed N to this N-limited system. Ultimately, all fixed N of the Pacific Arctic derives from northward flow through Bering Strait, both from the Alaska Coastal Water (ACW) to the east, and especially the nutrient-rich Anadyr water emanating from western Bering Strait (Walsh et al., 1989). However, in a given season, a large fraction of the available N may be locally regenerated from the shallow organic matter-rich sediments. Large fluxes of NH_4^+ out of sediments have been observed on the Chukchi shelf (Henriksen et al., 1993; Devol et al., 1997), providing evidence of local regeneration of N. Conversely, Horak et al. (2013) measured negligible fluxes of dissolved inorganic nitrogen (DIN, nitrate+nitrite+ammonium) from Bering shelf sediments, suggesting that local regeneration is not an important source of N. Resolving the role that sediments play in the local regeneration of N is crucial for understanding the nutrient dynamics of Western Arctic shelves.

Here, we use the stable isotopes of oxygen (^{16}O and ^{18}O) and nitrogen (^{14}N and ^{15}N) in NO_3^-, together with nutrient and dissolved gas tracers, to examine the marine N cycle from the Bering Strait, over the Chukchi shelf, and into the Canada Basin. Our discussion draws on the important study of Granger et al. (2011), which uses similar techniques in the Bering Sea to the south. We focus on both N loss processes and the origins of fixed N in this N-limited system. We give particular attention to the process of nitrification, which has received relatively little attention compared to denitrification, but which is central to the discussion of both N losses (through coupled nitrification-denitrification) and N sources (through local regeneration).

2. Methods

2.1. Field sampling and analysis

We collected water samples for nutrients, dissolved gases, and stable isotope analyses on three cruises aboard the USCGC *Healy* to the Chukchi/Beaufort seas. HLY1001 (June 15–July 22 2010) and HLY1101 (June 25–July 29 2011) comprised the field portion of the NASA program ICESCAPE (Impacts of Climate on the EcoSystems and Chemistry of the Arctic Pacific Environment) focused on the Chukchi Sea shelf, while HLY1003 (September 5–26, 2010) was a primarily mooring service cruise on which we accessed the deeper waters of the Canada Basin (Fig. 1).

At each station, water column profiles of temperature, salinity, and oxygen were measured using a Sea-Bird conductivity, temperature, and depth (CTD) system attached to a rosette. Water was collected at multiple depths into 30 L Niskin bottles. The temperature sensors underwent laboratory calibrations before and after the cruises, and the conductivity and oxygen sensors were calibrated at sea using water sample data.

Velocity measurements were obtained using the *Healy's* hull mounted Ocean Surveyor 150 kHz acoustic Doppler current profiler (ADCP). The data were acquired using the University of Hawaii's UHDAS software and underwent further processing with the CODAS3 software package (see http://currents.soest.hawaii.edu). The velocities were then de-tided using the Oregon State University model (http://volkov.oce.orst.edu/tides; Padman and Erofeeva, 2004). The accuracy of the final velocities is estimated to be ± 2 cm s^{-1}.

2.1.1. Nutrients

For ICESCAPE cruises HLY1001 and HLY1101, discrete water column samples were analyzed on-board with a Seal Analytical continuous-flow AutoAnalyzer 3 (AA3) for concentrations of NO_3^-, nitrite (NO_2^-), NH_4^+, and phosphate (PO_4^{3-}) using standard methods (Armstrong et al., 1967; Bernhardt and Wilhelms, 1967; Kerouel and Aminot, 1997). Nutrients from HLY1003 were frozen and analyzed using standard methods at the University of Alaska Fairbanks. Although freezing can affect measurements of NH_4^+ (Degobbis, 1973), we do not consider this to be problematic for two reasons: first, HLY1003 focused on off-shelf waters, which generally have very low NH_4^+ concentrations; second, our in-depth analyses of NH_4^+ (distribution, changes along the northward flow path, and comparison with isotopic data) were all done on the Chukchi shelf using ICESCAPE nutrient data which were not derived from frozen samples.

2.1.2. Stable isotopes of nitrate and water

Seawater samples were filtered through Sterivex filter units (0.22 μm pore size) into duplicate acid-rinsed 60 mL HDPE bottles, then frozen until analysis. $\delta^{15}N_{NO_3}$ and $\delta^{18}O_{NO_3}$ were measured using the denitrifier method (Sigman et al., 2001; Casciotti et al., 2002). Sufficient sample to yield 20 nmol NO_3 was added to an aliquot of culture containing denitrifying bacteria that lack N_2O reductase activity. The N_2O produced was analyzed by continuous flow isotope ratio mass spectrometry on a Thermo-Finnigan Delta^{PLUS} IRMS. Isotope ratios are reported using delta notation as follows:

$$\delta^{15}N_{NO_3}(‰) = \left[\left(^{15}N/^{14}N_{sample}\right)/\left(^{15}N/^{14}N_{standard}\right) - 1\right] \times 1000,$$

and

$$\delta^{18}O_{NO_3}(‰) = \left[\left(^{18}O/^{16}O_{sample}\right)/\left(^{18}O/^{16}O_{standard}\right) - 1\right] \times 1000$$

The $^{15}N/^{14}N$ reference standard is N_2 in air, while the $^{18}O/^{16}O$ reference standard is Vienna Standard Mean Ocean Water (VSMOW). Analyses were referenced to injections from a laboratory standard N_2O tank and standardized using reference materials USGS-32, USGS-34, and USGS-35 (Böhlke et al., 2003).

$\delta^{18}O_{H_2O}$ was measured as in Cooper et al. (2013), and is reported in the standard delta notation.

2.1.3. Particulate organic nitrogen

For ICESCAPE cruises HLY1001 and HLY1101, particulate organic nitrogen (PON) samples were collected for $\delta^{15}N$ analysis by filtering water samples onto pre-combusted (450 °C for 4 h) 25 mm Whatman GF/F filters (nominal pore size 0.7 μm). Filter blanks were produced by passing ~50 mL of 0.2 μm filtered seawater through a GF/F. All filters were then immediately dried

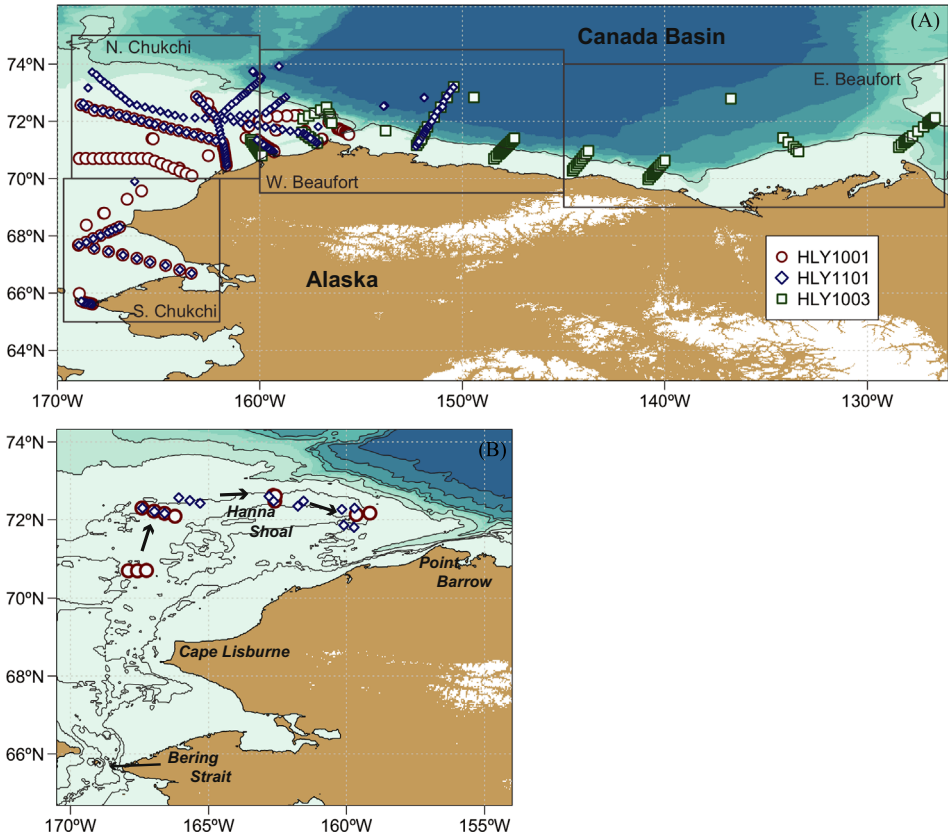

Fig. 1. Map of study region, showing all process stations from three separate research cruises in 2010–2011. (A) Boxes delineate regions of interest as described in Section 2.3. In (B), only stations comprising the main winter water (WW) flow path are shown (see Section 2), with arrows indicating the direction of flow.

at 60 °C and stored dry until analysis. Prior to analysis, samples and blanks were fumed with concentrated HCl, dried at 60 °C, and packed into tin capsules (Costech Analytical Technologies, Inc.) for elemental analysis on a Elementar Vario EL Cube (Elementar Analysensysteme GmbH, Hanau, Germany) interfaced to a PDZ Europa 20-20 isotope ratio mass spectrometer (Sercon Ltd., Cheshire, UK). We corrected for the filter blank by subtracting the mean blank PON concentration ($n=77$) from sample PON concentrations. We corrected $\delta^{15}N_{PON}$ (obtained for HLY1001 particulate samples only) for the filter blank using the method of Avak and Fry (1999).

2.2. Satellite sea ice data

Sea ice concentrations in the study region were determined from daily AMSR-E (Advanced Microwave Scanning Radiometer—Earth Observing System) data at 12.5 km resolution obtained from the National Snow and Ice Data Center (NSIDC). After projecting daily images onto an equal area grid of the Chukchi Sea, we determined the timing of sea ice retreat at each hydrographic station as the date when sea ice concentration first fell below 50%.

2.3. Definitions and calculations

From CTD data, we calculated potential temperature (θ, °C), potential density (σ_θ, km m^{-3}), and the square of the buoyancy frequency (N^2, s^{-2}) using the *oce* package version 4.0 of the statistical computing program R, version 2.13.0 (R Development Core Team, 2011). For each station, we used σ_θ to determine the thickness of the bottom layer, which we defined as all waters within 0.1 kg m^{-3} of the average σ_θ of the bottom 5 m (Fig. 2).

We computed N*, a measure of the excess fixed N over P (relative to Redfield proportions), as N* (μM)=($[NO_3^-]+[NO_2^-]+[NH_4^+]$)−16×$[PO_4]$+2.9 (Gruber and Sarmiento, 1997; Hirota et al., 2009; Granger et al., 2011). Apparent oxygen utilization (AOU) was calculated as the deficit in dissolved O_2 relative to saturation, using the software Ocean Data View version 4.3.10 (http://odv.awi.de).

We defined the continental shelf as having a water depth <200 m; stations deeper than this were considered off-shelf. For all Chukchi shelf water samples we focus on the deepest water sample taken at each hydrographic station. This was always within 3 m of the ocean bottom, as shown by the altimeter mounted on the rosette, and hence within the bottom layer as defined above. Throughout the text, the term "bottom waters" refers to the water comprising the bottom layer for the continuous CTD variables, or the deepest Niskin depth for the water sample variables.

We defined winter water (WW) on the Chukchi shelf as waters having temperature ≤ -1.6 °C and NO_3^- concentration ≥ 10 μM (the latter constraint is included to prevent surface meltwaters from being classified as WW). Using the WW distributions together with the ADCP velocity measurements, we mapped the dominant pathway of winter water over the Chukchi shelf in both 2010 and 2011 (Fig. 1B). This extends northward through the Central Channel and then bends anti-cyclonically around Hanna Shoal into Barrow Canyon. Hereafter we refer to this specific pathway as the "main WW flow path". Using the mean velocity of WW and the distance from Bering Strait, we determined how long waters at each station along the main WW flow path had been on the Chukchi shelf. This allowed us to calculate rates of change of chemical tracers in WW propagating along the main WW flow path across the Chukchi shelf.

To illustrate large-scale spatial patterns in N cycle tracers, we grouped our field samples into four regions of interest that broadly

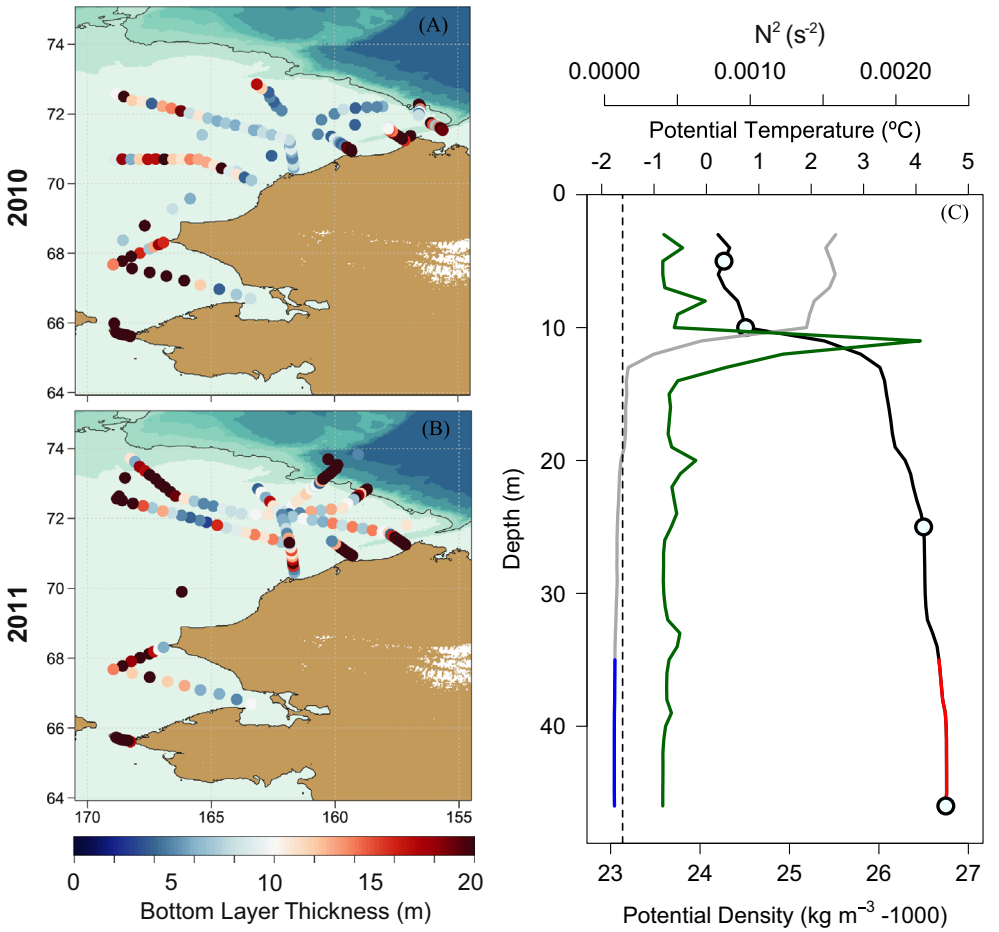

Fig. 2. Thickness of the bottom layer (the region within 0.1 kg m^{-3} of the average density of the bottom 5 m) across the Chukchi Shelf in (A) 2010 and (B) 2011. (C) A representative station along the main winter water flow path in 2010, with σ_θ shown in black (bottom layer in red), θ shown in grey (bottom layer in blue), and N^2 shown in green. The black circles denote the depths of Niskin bottle collection, and the dashed vertical line is $\theta = -1.6$ °C, which is defined as the upper interface of the winter water. (For interpretation of the references to color in this figure legend, the reader is referred to the web version of this article.)

define the general progression of WW from the Bering Strait to the Beaufort Sea (Fig. 1): from the Southern Chukchi Sea (Bering Strait to 70°N), to the Northern Chukchi Sea (north of 70°N and west of 160°W), to the Western Beaufort Sea (between 160°W and 145°W), and finally the Eastern Beaufort Sea (east of 145°W).

2.4. Source waters and water mass definitions

We defined Pacific source waters as the waters of the Bering Sea slope, identical to those used by Granger et al. (2011). These Bering slope waters upwell in the Gulf of Anadyr in the northern Bering Sea and flow northward through western Bering Strait, and are known to supply the vast majority (> 95%) of the NO_3^- flowing onto the Chukchi shelf (Walsh et al., 1989). Granger et al. (2011) defined these source waters as having a NO_3^- concentration of 20 μM, $\delta^{15}N_{NO_3} = 6.5‰$, and $\delta^{18}O_{NO_3} = 3.2‰$. This NO_3^- concentration roughly matches the Pacific source waters measured by Hansell et al. (1993) and Cooper et al. (1997).

Based on salinity, we defined waters of the Canada Basin as being either Pacific-origin ($S \leq 33.5$) or Atlantic-origin ($S \geq 34$) (Cooper et al., 1997; Hansell et al., 2004; Codispoti et al., 2005). Within the Pacific-origin waters, we defined the Pacific Upper-Halocline Layer (UHL) as having salinity between 32.5 and 33.5 (Hansell et al., 2004). The Pacific UHL contains the Pacific nutrient maximum and is generally considered to be centered on $S = 33.1$ (Cooper et al., 1997; Codispoti et al., 2005).

3. Results

3.1. Hydrographic conditions on the Chukchi Sea shelf

During the two ICESCAPE surveys, the density of surface waters averaged $\sigma_\theta \sim 24.3$. Bottom waters were relatively warm (> 0 °C, ranging up to > 6 °C) in the southern Chukchi Sea and along the Alaskan coast (Fig. 3A and B). However in the northern Chukchi Sea, bottom waters were very cold and significantly denser ($\sigma_\theta > 26.5$, Fig. 3A–D). These northern Chukchi Sea bottom waters were largely composed of WW that had not yet advected off the shelf at the time of sampling in June/July. In both 2010 and 2011, the maximum N^2 (a measure of water column stratification) was lowest near Bering Strait, indicating that these very shallow, energetic waters were well-mixed (Fig. 3E and F).

On the Chukchi shelf, surface DIN was generally already depleted by the time our sampling began in late June, averaging 0.31 ± 0.89 μM over 2010–2011. The few stations with surface DIN > 1 μM were mostly in the southwestern Chukchi Sea where we sampled the eastern edge of the nutrient-rich Anadyr water. Surface phosphate and silicate, however, were still at appreciable levels when surface DIN was depleted, averaging 0.56 ± 0.14 and 4.50 ± 4.85 μM, respectively. Bottom waters were far more nutrient-rich, containing 1.42 ± 0.49 μM phosphate, 20.9 ± 16.0 μM silicate, and 9.30 ± 6.21 μM DIN (maximum 21.6 μM). Of this DIN, 1.46 ± 1.13 μM (26% on average) was NH_4^+, while very little (0.11 ± 0.07 μM; 1.9% on average) was NO_2^-.

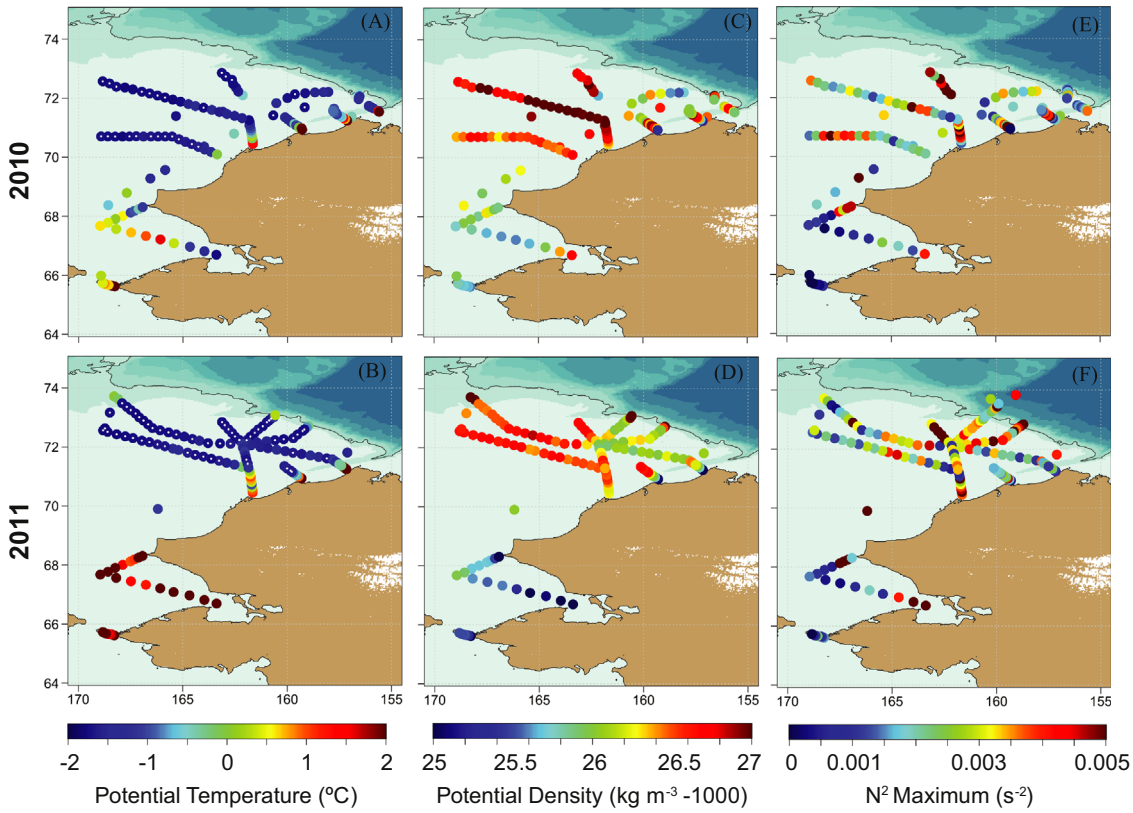

Fig. 3. (A) Average potential temperature (°C) and (B) potential density (σ_θ, kg m^{-3}) of bottom waters, and (C) the water column maximum of the square of the buoyancy frequency (N^2) at stations across the Chukchi shelf in summer 2010 and 2011. In panel (a), overlaid white dots indicate the distribution of winter water, as defined in the text.

There were strong positive correlations ($p < 0.001$) between all three forms of DIN (NO_3^-, NO_2^-, and NH_4^+) in bottom waters across the Chukchi shelf. Concentrations of all three were higher on the northern shelf than the southern shelf (Fig. 4). However, there were subtle differences in the distributions of these species: whereas NO_3^- was invariably depleted near the Alaskan coast – a region dominated by the warm, nutrient-poor Alaska Coastal Water in summer – NH_4^+ concentrations ranged up to 2 μM in these relatively warm coastal waters (Fig. 4C and D). NH_4^+ concentrations were generally very low in eastern Bering Strait, and in 2010, NH_4^+ was depleted north of Alaska in the region of Barrow Canyon. However, NH_4^+ could be detected over most of the Chukchi shelf, with concentrations ranging from ~0.5 to 6 μM (Fig. 4C and D). There was no clear pattern with latitude or with distance from the Alaska coast. NH_4^+ was highest in bottom waters in 83% of the shelf stations we sampled. We observed no significant relationship between NH_4^+ and phytoplankton biomass in bottom waters of the Chukchi shelf, either in terms of Chl *a* ($p = 0.117$) or PON ($p = 0.968$).

Dissolved O_2 concentrations in surface waters were generally supersaturated across the entire Chukchi shelf, averaging 113 ± 12% of saturation, and ranging up to 167% of saturation. Conversely, in bottom waters, dissolved O_2 concentrations decreased sharply from Bering Strait northward (Fig. 4E and F).

3.2. Nitrification rate calculation

We quantified AOU in bottom waters along the main WW flow path across the Northern Chukchi shelf (Fig. 1B). AOU increased from ~30 to ~90 μM over a period of ~50 days, although the increase in AOU was more robust in 2010 ($p < 0.01$) than in 2011 ($p = 0.05$) (Fig. 5A). The oxygen utilization rate (OUR, calculated as $\Delta AOU/\Delta t$) for an average main WW flow path bottom layer thickness of 10.3 m (nearly identical to that of Rowe and Phoel (1992); see Section 2) was 12.3 mmol O_2 m^{-2} d^{-1}. Finally, applying a remineralization ratio of (16 NO_3^-: −150 O_2) (Sarmiento and Gruber, 2006), we obtain a nitrification rate of 1.3 mmol N m^{-2} d^{-1}. The global remineralization ratio used in this calculation is within 4% of the value reported by Simpson et al. (2008) in the nearby Beaufort Sea and Amundsen Gulf. It is important to recognize that this stoichiometric method of calculating nitrification rate does not ignore other oxygen-consuming processes inherent in remineralization; the molar ratio we employ represents complete oxidation of organic matter into its constituent inorganic parts, which includes all steps of nitrification and all other processes of remineralization (see Sarmiento and Gruber, 2006, Chapter 4).

We also examined whether there were changes in NO_3^- or NH_4^+ along the main WW flow path reflecting this nitrification. NO_3^- concentrations exhibited no significant trend in either 2010 or 2011 ($p = 0.475$ and $p = 0.675$, respectively; Fig. 5B). There was a net decrease in NH_4^+ concentration along the main WW flow path in 2010, at a rate of 0.57 mmol N m^{-2} d^{-1} ($p = 0.001$), but not in 2011 ($p = 0.201$; Fig. 5C).

3.3. Hydrographic conditions in the Canada Basin

The off-shelf stations in the western and eastern Beaufort Sea (Fig. 1) from the September 2010 survey were used to assess conditions in the Canada Basin. This region has a significantly less dense surface layer (the Polar Mixed Layer Codispoti et al., 2005) than even the most buoyant surface waters of the Chukchi shelf (averaging $\sigma_\theta \sim 23.4$ and reaching $\sigma_\theta < 20$). This reflects the fact that, seaward of the Chukchi shelf, the isopycnals deepen beneath the Beaufort Gyre, which contains a pool of freshwater. In the Canada Basin, salinity increases sharply with depth (Fig. 6A) while potential temperature decreases with depth until reaching a

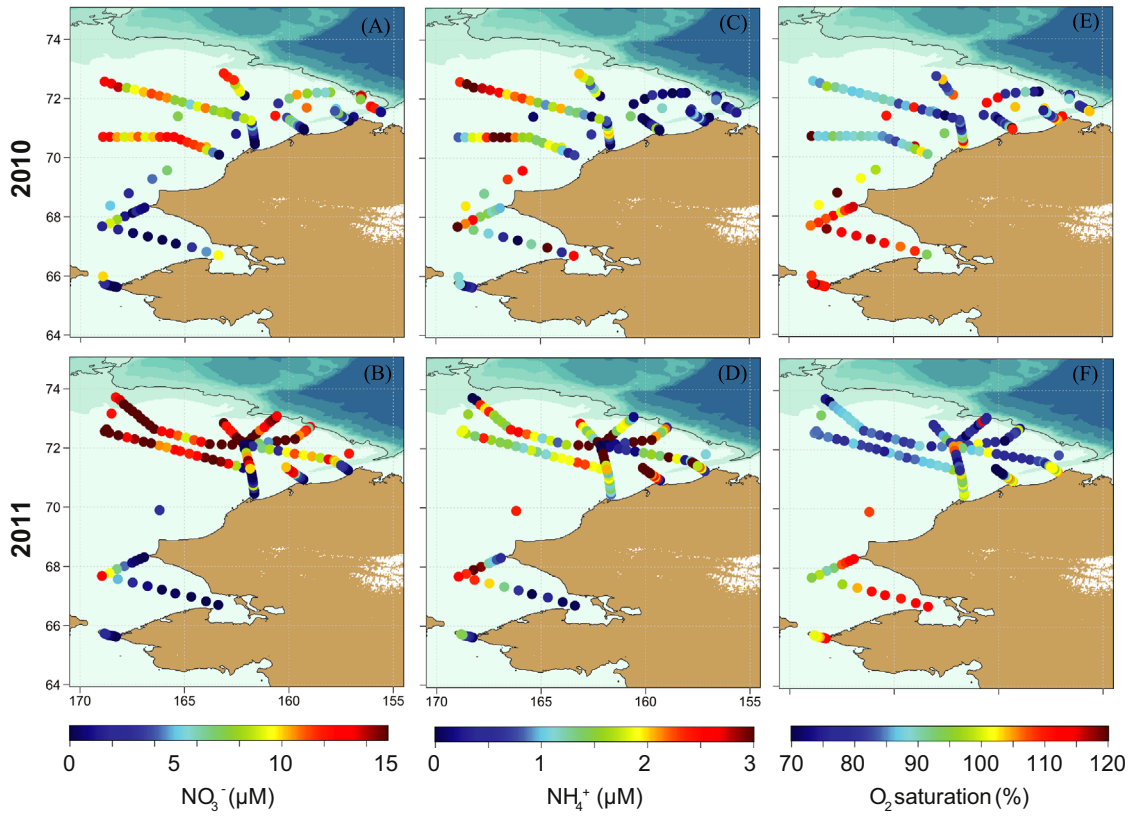

Fig. 4. Concentrations (μM) of (A) nitrate, (B) ammonium, and (C) dissolved oxygen saturation (%) in the bottom waters of the Chukchi shelf in summer 2010 and 2011.

minimum at ~150 m due to the remnant Pacific winter water that has fluxed off the shelf (e.g. Spall et al., 2008). This temperature minimum corresponds to a salinity of ~33.1 (Fig. 6B) within the Pacific Upper Halocline Layer (Aagaard et al., 1981; Codispoti et al., 2005). Below this layer, θ increases again, reaching an Atlantic-origin temperature maximum near a depth of ~450 m, below which θ decreases again to ~−0.5 °C in the Canada Basin Deep Water (CBDW).

Concentrations of both NH_4^+ and NO_2^- were very low in the Canada Basin (averaging 0.23 ± 0.45 and 0.07 ± 0.16 μM, respectively, at all depths). NO_3^- was fully depleted in the surface waters of the Canada Basin, and increased down to a nutrient maximum within the Pacific UHL, where it averaged 12.7 ± 1.8 μM (Fig. 6C, Table 1). The Pacific UHL was similar to bottom WW of the Chukchi shelf, both in terms of its salinity range (32.5–33.5) and its DIN concentration (Fig. 7). However, DIN in the Canada Basin was systematically higher than the warm (non-WW) bottom waters of the Chukchi shelf for any given salinity (Fig. 7).

3.4. Stable isotopes

$\delta^{18}O_{NO_3}$ decreased sharply in bottom waters across the Chukchi shelf, dropping from ~11‰ in Bering Strait to ~1‰ in the Barrow Canyon region (Fig. 8A). This ^{18}O-depleted NO_3^- near the Chukchi shelf break was typical of off-shelf, shallow Pacific-origin waters throughout our sampling area in the western and eastern Beaufort Sea, extending all the way to Amundsen Gulf, with $\delta^{18}O_{NO_3}$ averaging 1.1 ± 0.6‰ in the Pacific UHL (Fig. 6D). Meanwhile, $\delta^{18}O_{H_2O}$ averaged −1.4 ± 0.4‰ in bottom waters of the Chukchi shelf, similar to the value of −1.8 ± 0.2‰ in the Pacific UHL of the Canada Basin.

The oxygen isotopes of NO_3^- and H_2O allow us to separate the NO_3^- that ends up in the Pacific UHL ($NO_{3\,FINAL}^-$) into preformed NO_3^- ($NO_{3\,PRE}^-$; the fraction that flowed through Bering Strait and crossed the Chukchi Sea unaltered) and regenerated NO_3^- ($NO_{3\,REG}^-$, the fraction that was utilized by phytoplankton and was subsequently ammonified and nitrified), using an isotope mixing model:

$$[NO_{3\,PRE}^-]*\delta^{18}O_{NO3^-\,PRE}+[NO_{3\,REG}^-]*\delta^{18}O_{NO3^-\,REG} = [NO_{3\,FINAL}^-]*\delta^{18}O_{NO3^-\,FINAL} \quad (3.1)$$

Given an average $\delta^{18}O_{NO_3^-\,FINAL}$ of 1.1‰ in the Pacific UHL, and Bering slope source waters of 3.2‰ (Granger et al., 2011) (see Section 2), if we assume that the $\delta^{18}O$ of regenerated NO_3^- is equal to $\delta^{18}O_{H_2O}+1$ (Sigman et al., 2009; Granger et al., 2011) (−0.4‰ in our case), then 42% of the 12.7 μM NO_3^- in the Pacific UHL was preformed, while 58% was regenerated during the transit of Anadyr waters across the shelves of the Northern Bering and Chukchi Seas and/or in the Canada Basin, within the range observed by Granger et al. (2013) on the Bering Sea shelf.

Initially, $\delta^{15}N_{NO_3}$ also decreased moving northward from Bering Strait, falling from ~13‰ in Bering Strait to ~6‰ north of Cape Lisburne at 70–71°N (Fig. 8B). However, progressing further northward, $\delta^{15}N_{NO_3}$ began to rise again, reaching 8–9‰ in the vicinity of Barrow Canyon, the same region where bottom water NH_4^+ concentrations were reduced to near zero (Fig. 4C). Indeed, there was a strong negative correlation between NH_4^+ and $\delta^{15}N_{NO_3}$ in bottom waters of the Chukchi shelf ($p<0.001$). As NH_4^+ concentrations declined from >3 μM to ~0 μM, $\delta^{15}N_{NO_3}$ rose from 4–5‰ to 8–9‰ (Fig. 9). It was this relatively ^{15}N-enriched water that exited the shelf and typified shallow Pacific waters of the Canada Basin and Amundsen Gulf, which averaged 7.7 ± 0.3‰ in the UHL, ranging up to 8.2‰ (Fig. 6E).

In Pacific waters of the Chukchi shelf and Canada Basin, $\delta^{15}N_{NO_3}$ exhibited a significant negative relationship with DIN concentrations ($p<0.001$) and a significant positive relationship

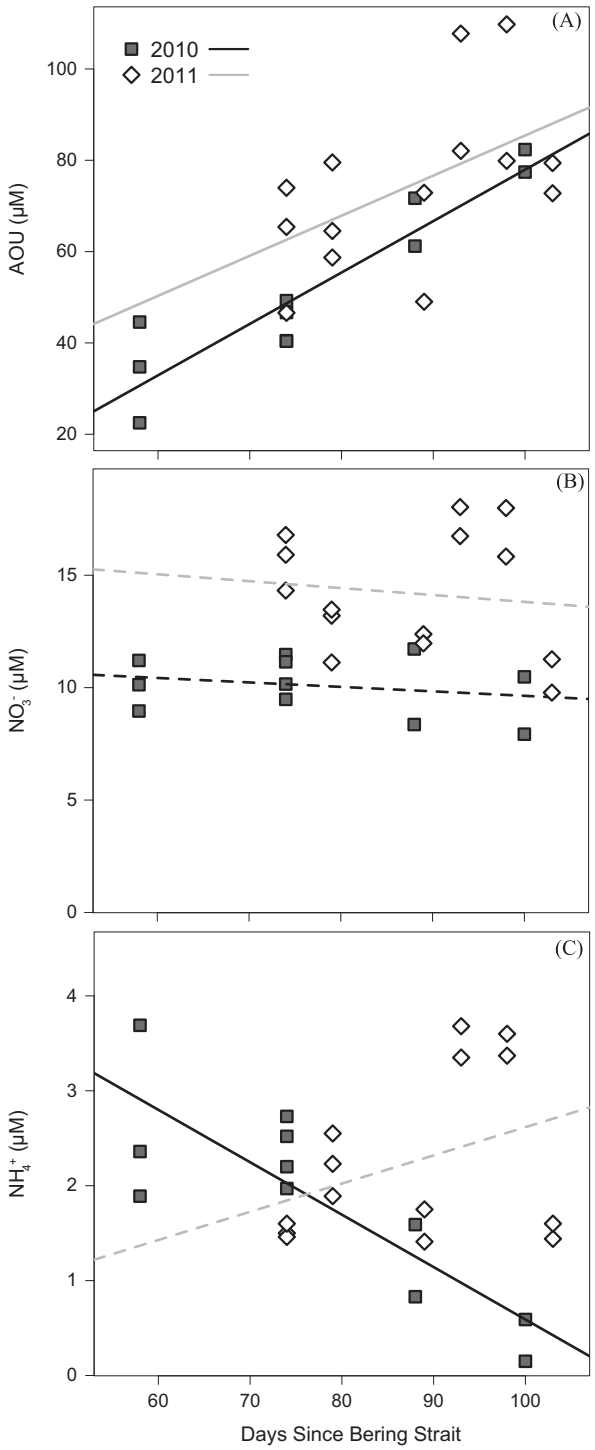

Fig. 5. (A) Apparent oxygen utilization (AOU), (B) NO_3^-, and (C) NH_4^+ in bottom waters of the main winter water flow path across the Chukchi shelf in summer 2010 and 2011. The *x*-axis shows the elapsed time since waters of each station flowed through Bering Strait, as estimated using ADCP data. Solid regression lines indicate statistical significance at the $p<0.05$ level; dashed regression lines indicate non-significance.

with N* ($p=0.014$) (not shown). $\delta^{18}O_{NO_3}$ did not exhibit significant relationships with either DIN concentration ($p=0.78$) or N* ($p=0.47$).

The NO_3^- of deep Atlantic-origin waters of the Canada Basin was isotopically distinct from that of shallow Pacific-origin waters (Fig. 6). Progressing to greater depth, $\delta^{15}N_{NO_3}$ decreased from 7.7 ± 0.3‰ in the Pacific UHL to 5.3 ± 0.3‰ in the Atlantic layer. In contrast, $\delta^{18}O_{NO_3}$ increased from 1.1 ± 0.5‰ in the Pacific UHL to 2.1 ± 0.4‰ in the Atlantic layer.

$\delta^{15}N_{PON}$ averaged 6.26 ± 2.95‰ for all sampling depths over the Chukchi shelf. We observed no relationship between $\delta^{15}N_{PON}$ and depth, and bottom data were not significantly different from surface data (Welch's *t*-test; $t=-0.83$; $p=0.41$). Furthermore, there was no significant relationship between $\delta^{15}N_{PON}$ and concentrations of NO_3^-, NO_2^-, NH_4^+, $\delta^{15}N_{NO_3}$, PON, Chl *a*, or N* in either bottom or surface waters. In low Chl *a* samples (<2 μg L^{-1}), $\delta^{15}N_{PON}$ was poorly constrained, ranging from <-5 to >15‰ and averaging 5.78 ± 3.33‰. However, at high Chl *a* concentrations (>17 μg L^{-1}, $n=40$), $\delta^{15}N_{PON}$ was much more uniform, ranging from 5.8 to 8.8‰, averaging 7.20 ± 0.80‰ (Fig. 10).

4. Discussion

4.1. Phytoplankton uptake signal in bottom waters of the southern Chukchi Sea

Sea ice retreats northward from the Bering Sea across the Chukchi shelf throughout the spring and early summer, stimulating phytoplankton production in surface waters. The ice edge typically passes through Bering Strait in mid-late May, and by the time of our sampling in 2010 and 2011 (June–July), most of the Chukchi shelf was ice-free. Thus, the phytoplankton bloom in the Chukchi Sea was well underway, explaining our observation of significant NO_3^- reduction and O_2 supersaturation in surface waters across the Chukchi shelf. Interestingly, in the southern Chukchi Sea, we also observed evidence of phytoplankton growth (low NO_3^-, high O_2) in bottom waters (Fig. 4), where phytoplankton growth should be negligible due to insufficient light.

The low NO_3^- and high O_2 in bottom waters of the southern Chukchi Sea results from energetic currents and tides in and around Bering Strait that completely mix the shallow (~50 m) water column, giving this region the lowest N^2 maxima on the Chukchi shelf (Fig. 3E and F). As Bering Strait waters subsequently flow northward, they stratify, effectively trapping bottom waters beneath the pycnocline where algal growth ceases, yet these bottom waters still harbor a remnant algal growth signal that was generated in and around Bering Strait. By July, this remnant algal growth signature in bottom waters penetrated northward into well-stratified areas of the shelf as far as Cape Lisburne (Figs. 4 and 8). Beyond that point the remnant algal growth signal diminished in intensity (Figs. 4 and 8), because more distant water parcels flowed through Bering Strait earlier in the season prior to the phytoplankton bloom. Therefore, this algal growth signal did not affect O_2 and nutrient calculations along the main WW flow path, which was entirely north of Cape Lisburne on the northern Chukchi shelf (Fig. 1).

This phytoplankton uptake signal in bottom waters of the southern Chukchi shelf explains the counter-intuitive pattern of bottom water NO_3^- increasing to the north across the Chukchi shelf from Bering Strait to the shelf break (Fig. 4A and B), seemingly at odds with the strong denitrification known to occur on the Chukchi shelf. In addition, it explains the isotopic enrichment of NO_3^- in bottom waters of the southern Chukchi shelf (Fig. 8). Because phytoplankton utilizing NO_3^- discriminate against the heavy isotopes of both N and O, phytoplankton uptake enriches the residual NO_3^- pool in ^{15}N and ^{18}O in approximately a 1:1 relationship (Granger et al., 2004; Karsh et al., 2012). In the bottom waters of Bering Strait, we observed a maximum NO_3^- concentration of only 2.7 μM and $\delta^{15}N_{NO_3}$ and $\delta^{18}O_{NO_3}$ were at their highest

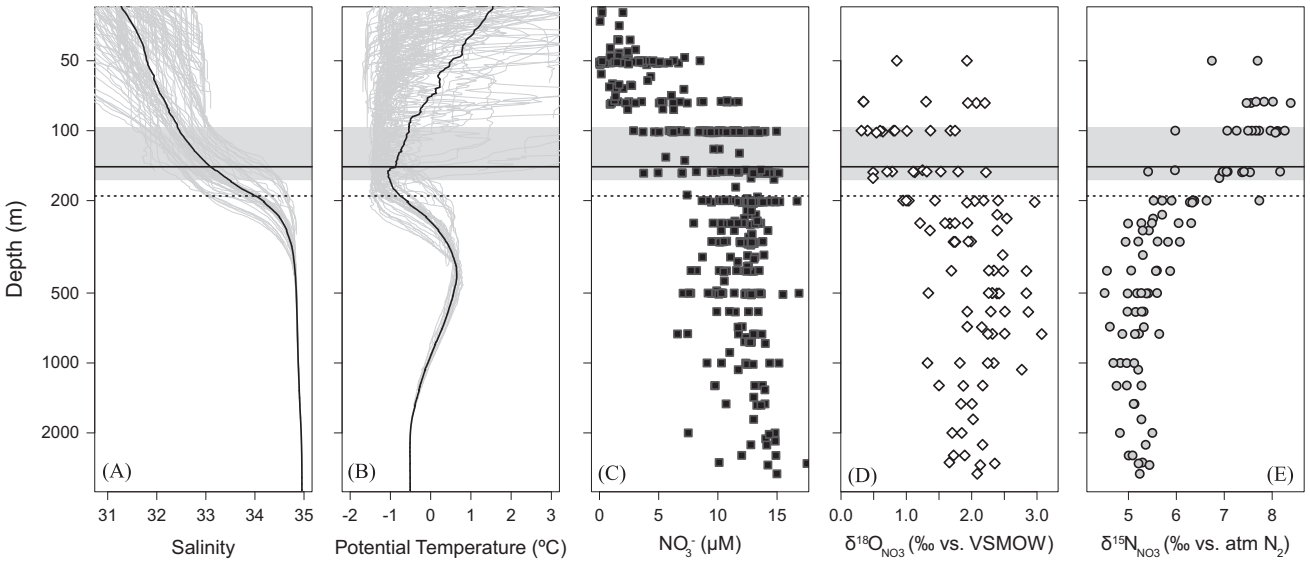

Fig. 6. Depth profiles of (A) salinity, (B) potential temperature (θ), (C) nitrate concentration, (D) $\delta^{18}O_{NO_3}$ and (E) $\delta^{15}N_{NO_3}$ in the off-shelf (> 200 m depth) waters of the Canada Basin from the September 2010 *Healy* cruise. In (A) and (B), light grey lines show all CTD casts, while thick black line shows the average profile over all stations. In all panels, the grey shaded region indicates the Pacific Upper Halocline Layer (UHL; $32.5 \le S \le 33.5$), and the solid line within it indicates $S = 33.1$, generally taken as the center of the UHL. The dotted line indicates $S = 34$, below which we consider to be Atlantic-origin waters.

Table 1
Properties of NO_3^- in the waters of the Bering Sea slope, Chukchi shelf winter waters, and Chukchi Sea slope (mean ± standard deviation).

	Bering Sea slope[a]	Chukchi shelf winter waters	Chukchi Sea slope
NO_3^- concentration (μM)	20	13.8 ± 2.5	12.7 ± 1.8
$\delta^{15}N_{NO_3}$ (‰)	6.5	5.7 ± 0.9	7.7 ± 0.3
$\delta^{18}O_{NO_3}$ (‰)	3.2	2.6 ± 0.9	1.1 ± 0.6

[a] *Source*: Granger et al. (2011).

levels anywhere on the shelf, reaching 13‰ and 11‰, respectively (Figs. 8 and 11)—a signal of intense algal growth.

These bottom waters of the southern Chukchi Sea, carrying their signal of phytoplankton uptake, eventually sweep out into the Canada Basin, likely in the fall. Interestingly, in addition to having very low nutrients, these waters also have very low density ($\sigma_\theta < 26$; Fig. 3C and D) likely due to both warming (from mixing into the surface layer near Bering Strait) and reduced salinity (due to freshwater input from both ice melt and the Yukon River). Because ocean waters tend to flow along isopycnal surfaces, waters of a given density flowing across the Chukchi shelf will partition themselves into the vertical density structure of the Canada Basin (which is perennially stable due to extreme salinity stratification). Whereas the dense, high-NO_3^- WW of the northern Chukchi shelf (with $\sigma_\theta \sim 26.5$; Fig. 3C and D) will find an equilibrium depth in the Canada Basin of ~130–150 m (within the Pacific UHL), the buoyant, low-NO_3^- bottom waters of the southern Chukchi shelf (with $\sigma_\theta \sim 25.6$) will end up at a much shallower equilibrium depth of ~50–80 m. Although these buoyant, nutrient-deprived summer waters flow through Bering Strait for only a fraction of the year, their volume flux is large. Woodgate et al. (2012) estimate that roughly equal volumes of winter and summer waters flow through Bering Strait, eventually entering the Canada Basin at very different depths. Thus, the fact that phytoplankton uptake reaches the bottom in summer in well-mixed Bering Strait, stripping nutrients from the entire low-density summer water column, contributes to the perennially low nutrient concentrations in the strongly-stratified upper Canada Basin.

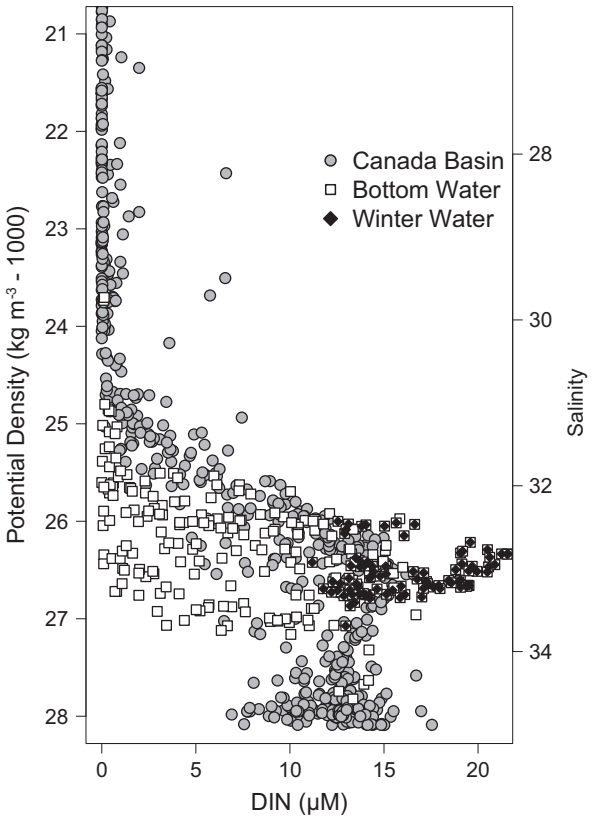

Fig. 7. Dissolved inorganic nitrogen (DIN) plotted against potential density (σ_θ) for the bottom waters of the Chukchi shelf and for all waters in the Canada Basin. Those stations on the Chukchi shelf containing winter water are highlighted.

4.2. NH_4^+ build-up on the Chukchi Sea shelf

A prominent and consistent feature of shallow Arctic shelves is the build-up of substantial amounts of NH_4^+ (Codispoti et al., 1991), which has been observed on both the Bering shelf (Whitledge et al., 1986; Granger et al., 2011; Horak et al., 2013) and the Chukchi shelf (Cooper et al., 1997; Codispoti et al., 2005,

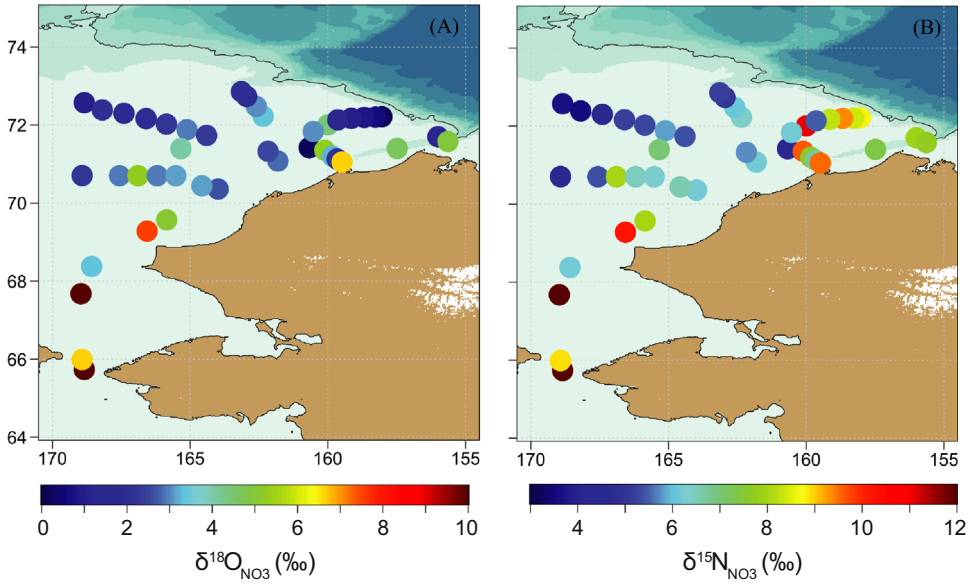

Fig. 8. (A) $\delta^{18}O_{NO_3}$ and (B) $\delta^{15}N_{NO_3}$ (‰) in bottom waters of the Chukchi shelf in June–July 2010.

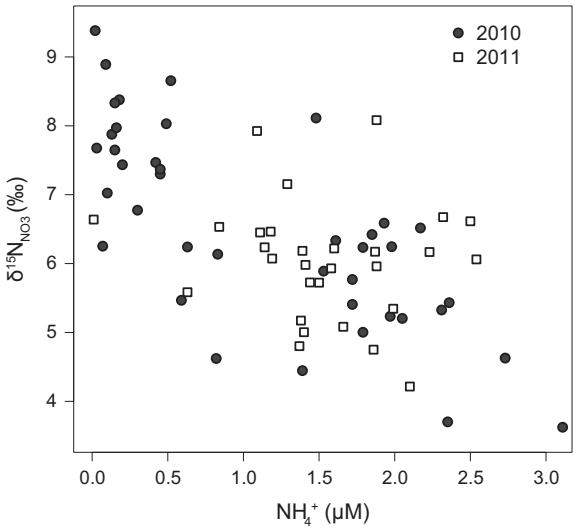

Fig. 9. $\delta^{15}N_{NO_3}$ versus ammonium concentration in bottom waters of the Chukchi shelf on the ICESCAPE cruises in 2010 and 2011.

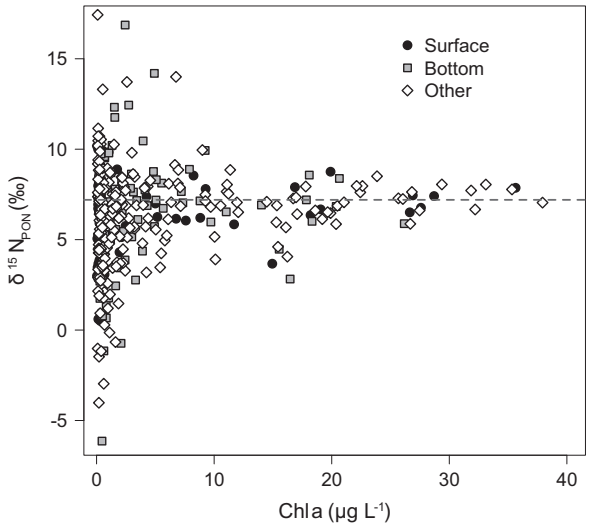

Fig. 10. $\delta^{15}N_{PON}$ versus Chl *a* concentration for samples in waters of the Chukchi shelf, partitioned into bottom samples, surface samples, and samples at intermediate depth. The horizontal dashed line shows $\delta^{15}N_{PON}$=7.2‰, the average for samples with high biomass (> 17 μg L^{-1} Chl *a*).

2009). On ICESCAPE, we observed accumulations of NH_4^+, averaging 2.1 μM in bottom WW and building up to 5.7 μM, similar to the average of 2.5 μM observed by Cooper et al. (1997). This implies a decoupling in the marine N cycle, in which NH_4^+ is liberated from organic matter more rapidly than it is utilized for growth or oxidized to NO_2^- and then to NO_3^-. Therefore, this NH_4^+ build-up is fundamentally important to the N cycle on continental Arctic shelves, yet it is not well-understood.

Shelf sediments are a possible source of NH_4^+. Because of the extremely high seasonal productivity of the shallow Chukchi Sea, a great deal of organic matter reaches shelf sediments and is subsequently ammonified. Early work showed strong fluxes of NH_4^+ out of sediments (0.7–1.2 mmol m^{-2} d^{-1}) on the Bering and Chukchi shelves (Lomstein et al., 1989; Henriksen et al., 1993; Devol et al., 1997). However, more recently, Horak et al. (2013) observed negligible fluxes of DIN out of Bering Sea sediments, suggesting that NH_4^+ accumulations must have originated from organic matter within the water column. Although we did not measure sediment nutrient fluxes, our observation that NH_4^+ concentrations were highest at the bottom in 83% of shelf stations suggest that the main source of NH_4^+ in the Chukchi Sea is likely to be shelf sediments. It is unlikely that this bottom water NH_4^+ was primarily generated from bloom organic matter in the water column, as this material had generally not yet reached bottom waters at the time of our sampling, with maximum PON concentrations being above the bottom layer in 74% of stations. Furthermore, as will be discussed below (Section 4.4), the mechanism of N isotopic enrichment that we observed on the Chukchi shelf and Granger et al. (2011) observed on the Bering shelf requires a sedimentary source of NH_4^+. Hence, we conclude that shelf sediments are the primary source of NH_4^+ in the Chukchi Sea.

The seasonal cycle of NH_4^+ accumulation is also poorly understood because few winter nutrient data exist in Arctic waters. However, in their study of the annual cycle of nutrients on the Bering shelf, Whitledge et al. (1986) provide compelling evidence that NH_4^+ accumulates in bottom waters only in summer (their Fig. 7), a conclusion supported by the modeling study of Deal et al. (2008). Likewise, Codispoti et al. (2005, 2009) and Mordy et al. (2012) observed far lower NH_4^+ concentrations in spring than

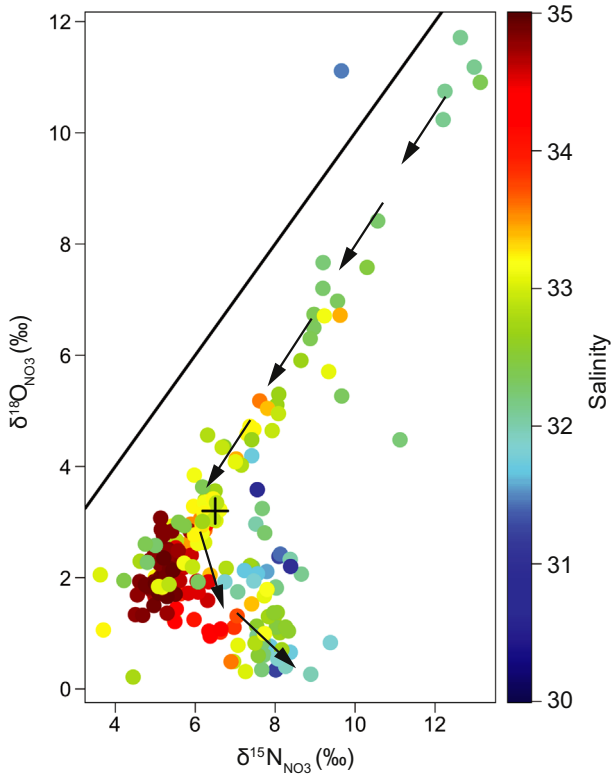

Fig. 11. $\delta^{18}O_{NO_3}$ versus $\delta^{15}N_{NO_3}$ in the Chukchi Sea and Canada Basin, colored by salinity. The 1:1 line is shown, and Bering Slope source waters (Granger et al., 2011) are shown with a cross. Arrows show the direction of flow of Pacific-origin water. (For interpretation of the references to color in this figure legend, the reader is referred to the web version of this article.)

summer on the Chukchi and Bering shelves, respectively. Thus, the preponderance of evidence suggests that NH_4^+ concentration is low in winter and that NH_4^+ accumulates in summer. Because NH_4^+ concentrations reflect the relative rates of supply and loss processes, this immediately raises the question of whether NH_4^+ concentration rises in summer due to relatively rapid ammonification, slower NH_4^+ oxidation, or both.

Whitledge et al. (1986) ascribe this seasonal buildup of NH_4^+ to the input of spring bloom organic matter during the growth season, and thus enhanced rates of ammonification. In addition, recent work suggests that nitrification of this NH_4^+ actually slows in summer. Christman et al. (2011) concluded, based on the abundance of *amoA* (the gene responsible for NH_4^+ oxidation), that the potential nitrification rate was >20-fold higher in winter than summer in shallow waters near Point Barrow. This was recently confirmed by an annual study in the same region, which found that nitrification rates were 21.6 nmol N L^{-1} h^{-1} in winter compared to only 1.0 nmol N L^{-1} h^{-1} in summer (Baer et al., unpublished manuscript). It is unclear how representative these studies are of the broader Chukchi shelf because nitrifiers in the very shallow (<10 m), near-shore waters of these studies may be especially prone to light inhibition and competition with primary producers for NH_4^+ in summer, perhaps restricting their rates more than in deeper parts of the shelf.

Our data support the notion that nitrification slows in summer. First, as noted above (and similar to Granger et al. (2011)), we observe NH_4^+ build-ups in bottom waters prior to the input of large amounts of bloom organic material to bottom waters, making it unlikely that enhanced ammonification is primarily responsible. Second, we observed that the "oldest" waters on the Chukchi shelf (i.e. those that passed through Bering Strait earliest in the year, which we sampled near Barrow Canyon in 2010) had no NH_4^+, and also had the lowest $\delta^{18}O_{NO_3}$ we observed on the shelf (<1.5‰; Figs. 4C, 8A), a clear signal of nitrification, as discussed below in Section 4.4. This is consistent with high rates of winter nitrification that do not permit build-ups of NH_4^+ on the shelf. Thus, we suggest that NH_4^+ is continually supplied to the Chukchi shelf bottom waters from organic matter-laden sediments, but that it only accumulates in summer when nitrification rates are lower than remineralization rates. Annual time series of nutrients and nitrification rates over the Chukchi shelf would be extremely useful to test this hypothesis.

4.3. Sediment vs. water column nitrification on the Chukchi Sea shelf

While the Chukchi Sea's broad, shallow, productive shelf is known to fuel a significant fraction of marine denitrification (Chang and Devol, 2009), nitrification is also likely to play an important role in the N cycle dynamics of this region. For example, on the Bering shelf to the south, nitrification was recently shown to provide NO_3^- substrate to fuel denitrification (Horak et al., 2013), as well as resupplying up to 100% of the NO_3^- to the inner shelf water column, fueling primary production (Granger et al., 2011). In addition, as described above, nitrification may have important seasonal dynamics, affecting concentrations of NH_4^+. Thus, it is important to further our understanding of nitrification on the adjacent Chukchi shelf, which has received little attention to date.

Because nitrification consumes O_2, we were able to infer rates of nitrification based on the removal of O_2 (i.e. increasing AOU) along the main WW flow path across the northern Chukchi shelf in both 2010 and 2011 (Figs. 1B, 5A). The dramatic increase in AOU in bottom waters of the main WW flow path (Fig. 5A) points to a strong signal of remineralization of organic matter, from which we estimated a nitrification rate of 1.3 mmol N m^{-2} d^{-1}. An important question is whether this O_2 consumption and concomitant nitrification occurs primarily in the sediments or the water column of the Chukchi Sea. Both sedimentary and bottom water nitrification draw O_2 from bottom waters; thus our bottom water O_2 measurements integrate both rates and cannot distinguish between the two. As will be discussed below, sedimentary and water column nitrification must both be occurring because both are essential to explain the ^{15}N enrichment of NO_3^- we observed in the Canada Basin. Parsing nitrification into sediment and water column contributions would aid our understanding of coupled nitrification-denitrification in the sediments and the cause of NH_4^+ build-ups in the water column.

We used NH_4^+ and NO_3^- changes along the main WW flow path to assess the importance of water column nitrification, which should decrease NH_4^+ concentrations and increase NO_3^-. It should be noted that changes in NH_4^+ and NO_3^- concentrations reflect not only water column nitrification but also sediment fluxes, the possible effect of which is addressed below. In 2010, we observed evidence of water column nitrification in the main WW flow path, as NH_4^+ was drawn down in bottom waters at a rate of 0.57 mmol m^{-2} d^{-1} (Fig. 5C), accounting for perhaps ~44% of our total nitrification rate of 1.3 mmol m^{-2} d^{-1} (see also Section 4.4). However, in 2011 we observed no such NH_4^+ drawdown, and in neither year did we observe an increase in NO_3^- along the main WW flow path that would indicate active water column nitrification (Fig. 5B). These results suggest that at the time of sampling in 2010, water column nitrification may still have been significant, but in 2011 when we sampled later in the summer, the bulk of O_2 drawdown and nitrification activity may have been in the sediments.

The O_2 demand and nitrification rates we observed match well with historically measured sedimentary rates. Our O_2 consumption rate of 12.3 mmol m^{-2} d^{-1} fits within the range of sediment O_2

demand measured previously on the Chukchi shelf, which is generally 5–13 mmol O_2 m^{-2} d^{-1} in Alaska Coastal Water (ACW), and 16–20 mmol O_2 m^{-2} d^{-1} in Bering Shelf-Anadyr Water (BSAW) (Grebmeier and McRoy, 1989; Henriksen et al., 1993; Devol et al., 1997). The correspondence of these rates suggests that the organic matter-rich sediments of the Chukchi shelf indeed draw their O_2 from the bottom waters flowing over them, that sediment O_2 demand is reflected in these bottom waters as they traverse the shelf northward, and that during the time of our sampling (especially in 2011), most remineralization on the shelf may have occurred in sediments rather than in the lower water column. Furthermore, the nitrification rate we estimate is similar to the sediment nitrification rate of 1.0–1.2 mmol N m^{-2} d^{-1} measured by Henriksen et al. (1993) in the southern Chukchi Sea, and within the range of shelf sediment nitrification rates of 0.7–1.8 mmol N m^{-2} d^{-1} given in the review of Henriksen and Kemp (1988). Thus, the correspondence of our estimated nitrification rate to previously measured sedimentary nitrification rates further suggests that most of the O_2 loss along the main WW flow path was driven primarily by nitrification in sediments, rather than in the water column.

An alternative explanation for the NH_4^+ and NO_3^- patterns that we observe along the main WW flow path is that there is significant water column nitrification, but its effects are masked by sediment nutrient fluxes. For example, a water column nitrification rate of 0.7 mmol m^{-2} d^{-1} could be hidden by a simultaneous NH_4^+ input from sediments of 0.7 mmol m^{-2} d^{-1} (Lomstein et al., 1989; Devol et al., 1997) and a simultaneous NO_3^- flux to sediments of 0.7 mmol m^{-2} d^{-1}, potentially explaining why we observe no significant changes in these nutrients along the main WW flow path in 2011 (Fig. 5B and C). However, this explanation requires strong fluxes of NO_3^- to the sediments, which are generally not observed (Lomstein et al., 1989; Henriksen et al., 1993). Thus, the most parsimonious explanation is that water column nitrification was low at the time of our sampling (particularly in 2011 when we observed no net changes in NH_4^+ or NO_3^- along the main WW flow path) with most nitrification and O_2 demand being sediment-driven.

Interestingly, our estimated nitrification rate of 1.3 mmol m^{-2} d^{-1} is similar in magnitude to sediment denitrification rates measured on western Arctic shelves. Devol et al. (1997) found average Chukchi Sea denitrification rates of 1.3 and 1.4 mmol N m^{-2} d^{-1} using two separate methods, similar to the 1.4 mmol N m^{-2} d^{-1} measured in BSAW sediments of the Chukchi Sea by Henriksen et al. (1993), and the 1.0 mmol N m^{-2} d^{-1} recently measured across the Chukchi Sea by Chang and Devol (2009). It is also similar to denitrification rates measured on the Bering shelf by Tanaka et al. (2004) (0.7–1.5 mmol N m^{-2} d^{-1}) and Horak et al. (2013) (0.86–1.19 mmol N m^{-2} d^{-1}). The similarity of our estimated (primarily sedimentary) nitrification rates to historically measured denitrification rates suggests a mechanistic coupling between these two processes; i.e. nitrification fuels denitrification in sediments, as described below.

4.4. Coupled partial nitrification-denitrification (CPND)

Given that primary production in the Western Arctic is strongly N limited in summer, it is important to understand whether fixed N is primarily lost to microbial activity in anoxic sediments through (1) direct flux of NO_3^- from the water column, or (2) NO_3^- remineralized from organic matter in overlying oxic sediments. The first mechanism, direct NO_3^- flux, is unlikely to play a large role in the Chukchi shelf region, as previous work shows that NO_3^- fluxes into sediments are very small or negative (i.e. out of sediments) on the Bering and Chukchi shelves (Henriksen et al., 1993; Devol et al., 1997; Rowe and Phoel, 1992; Horak et al., 2013). The second mechanism of NO_3^- supply to anoxic sediments, termed coupled nitrification-denitrification, has been shown to be of primary importance in coastal Greenland sediments (Rysgaard et al., 1998) and on the Bering shelf (Horak et al., 2013).

Granger et al. (2011) recently showed that on the Bering shelf, this process of nitrification fueling denitrification leads to ^{15}N-enrichment of water column fixed N. In this process, sediment organic matter in the shallow shelf sediments is ammonified by heterotrophic bacteria and macrofauna. A portion of the resulting NH_4^+ (~5% in the study of Granger et al. (2011)) is nitrified in sediments with a substantial isotope effect, thus producing relatively ^{15}N-depleted NO_3^- that becomes substrate for denitrification to N_2 gas in the anoxic sediments. This coupled partial nitrification-denitrification removes isotopically light fixed-N from the system. The remainder of the sedimentary NH_4^+, which is ^{15}N-enriched due to the same partial nitrification process, may diffuse out of sediments and ultimately become nitrified in the water column, thereby enriching $\delta^{15}N_{NO_3}$. The net effect of this coupled partial nitrification-denitrification (CPND) is to preferentially remove isotopically light fixed-N from the system through denitrification, enriching the remaining fixed-N pool (Granger et al., 2011).

Our NO_3^- stable isotope data strongly support the presence of CPND on the Chukchi shelf. North of Cape Lisburne (i.e. beyond the reach of the phytoplankton uptake signal that dominates the southern Chukchi shelf), $\delta^{15}N_{NO_3}$ increases northward from <6 to >8‰, becoming significantly enriched relative to Bering slope source waters (6.5‰, Table 1, Granger et al., 2011). This is consistent with the mechanism of CPND, which releases relatively enriched NH_4^+ from sediments that is ultimately nitrified in the water column. This accounts for our observation that $\delta^{15}N_{NO_3}$ rises as NH_4^+ concentration falls (Fig. 9), as was also observed by Granger et al. (2011) (their Fig. 6). The elevated $\delta^{15}N_{NO_3}$ value observed once NH_4^+ is completely converted to NO_3^- implies that the NH_4^+ pool was relatively enriched in ^{15}N, which we would expect based on partial sedimentary nitrification. Specifically, taking our WW averages on the Chukchi shelf of $[NO_3^-]=13.8$, $[NH_4^+]=2.1$, and $\delta^{15}N_{NO_3}=5.7$‰, and assuming that all NH_4^+ has been converted to NO_3^- in Canada Basin samples with $\delta^{15}N_{NO_3}=7.7$‰ , this implies that $\delta^{15}N_{NH_4}$ in Chukchi Sea WW was 20.8‰ (similar to the steady state value of 17‰ in Granger et al. (2011)). This is far heavier than the $\delta^{15}N$ of the organic matter ($\delta^{15}N_{PON}$) from which this NH_4^+ was produced (~7.2‰, Fig. 10), despite the fact that ammonification and flux to the water column are not thought to have substantial isotope effects (Granger et al., 2011). This ^{15}N enrichment of NH_4^+ relative to organic matter was likely a result of CPND in sediments, which preferentially removed light NH_4^+.

As $\delta^{15}N_{NO_3}$ became enriched, $\delta^{18}O_{NO_3}$ simultaneously decreased from ~3 to ~1‰ (Fig. 8), becoming significantly ^{18}O-depleted compared to its Bering slope source waters (3.2‰ Granger et al., 2011). This change is also consistent with CPND. The process of nitrification produces NO_3^- with $\delta^{18}O$ similar to that of H_2O (Buchwald et al., 2012), which is extremely ^{18}O-depleted in the bottom waters of the Chukchi shelf (averaging −1.4‰), owing to ice and river influences. Thus, the observed reduction of $\delta^{18}O_{NO_3}$ across the Chukchi shelf arises from the introduction of ^{18}O-depleted newly nitrified NO_3^-, as we would expect from CPND.

Granger et al. (2011) pointed out that the ^{15}N enrichment of NO_3^- could be due to partial denitrification in sediments followed by the flux of enriched residual NO_3^- into bottom waters. However, several lines of evidence rule out this possibility. First, previous work shows that while NH_4^+ fluxes out of shelf sediments can be substantial, NO_3^- fluxes from the sediments are very low (Lomstein et al., 1989; Henriksen et al., 1993). Thus, it is likely that the $\delta^{15}N_{NO_3}$ enrichment is driven by ^{15}N-enriched NH_4^+ from sediments, rather than

^{15}N-enriched NO_3^-. Second, if partial denitrification were the cause of the enrichment, there would be a negative relationship between N* and $\delta^{15}N_{NO_3}$ (i.e. as N is removed by partial denitrification, it leads to isotopic enrichment of residual NO_3^-). However, we did not observe this relationship; instead, we observed a highly significant relationship between NH_4^+ concentration and $\delta^{15}N_{NO_3}$ (Fig. 9), showing that the ^{15}N enrichment is directly connected to nitrification, not denitrification. Third and most importantly, partial denitrification should simultaneously enrich both $\delta^{15}N_{NO_3}$ and $\delta^{18}O_{NO_3}$ (Granger et al., 2011), which is not what we observed. Instead, $\delta^{18}O_{NO_3}$ decreased to the north as $\delta^{15}N_{NO_3}$ increased, indicative of accumulation of regenerated NO_3^-. Therefore, we conclude, as did Granger et al. (2011) for the Bering Sea, that CPND, rather than partial denitrification, is most likely responsible for the ^{15}N enrichment of NO_3^- on the Chukchi shelf and in the Canada Basin.

It is important to note that both sediment and water column nitrification are integral to the CPND mechanism for $\delta^{15}N_{NO_3}$ enrichment, yet our O_2 and nutrient data primarily show evidence of sedimentary nitrification at the time of our sampling, especially in 2011 (see Section 4.3). Resolving this apparent contradiction likely involves the rate of water column nitrification, which may be particularly slow in summer, as discussed in Section 4.2. First, although tracers along the main WW flow path point primarily to sediment nitrification, there is evidence of a modest amount of water column nitrification on the Chukchi shelf. In WW, NO_3^- was ^{18}O-depleted relative to Bering slope source waters (Table 1), indicating input of some fresh NO_3^-. Similarly, WW NO_3^- was ^{15}N-depleted compared to source waters, which is also indicative of nitrification. Drawing from a ^{15}N-enriched NH_4^+ pool with $\delta^{15}N_{NH_4}$ of ~21‰, given an isotope effect of 15‰ (Granger et al., 2011), the first newly nitrified NO_3^- would have $\delta^{15}N < 6$‰, tending to initially deplete $\delta^{15}N_{NO_3}$, as we observed (as nitrification goes to completion, it will eventually enrich $\delta^{15}N_{NO_3}$). Thus, Chukchi Sea WW bears a signal of modest water column nitrification. The clearest evidence of water column nitrification on the Chukchi shelf comes from 2010 near Point Barrow, at the end of the main WW flow path, where NH_4^+ concentration was drawn down to near zero, $\delta^{15}N_{NO_3}$ had climbed to >8‰, and $\delta^{18}O_{NO_3}$ had dropped to ~1‰ (Figs. 4C, 5C, 8), all of which are consistent with water column nitrification and CPND. There is no comparable signal on the Chukchi shelf in 2011, possibly because nitrification rates are lower in summer; earlier sea ice retreat (by >2 weeks) and later sampling in 2011 meant that the summer season was at least 1 month further advanced at the time of sampling in 2011, such that we may have captured only the slower water column nitrification rates of summer.

Although water column nitrification may be very slow on the Chukchi shelf in summer (thus allowing significant accumulations of NH_4^+ to develop), it will nonetheless go to completion after these waters sweep into Canada Basin, thus losing contact with the sediments and eliminating the source of fresh NH_4^+. Supporting this view, Codispoti et al. (2005, 2009) observed NH_4^+ plumes extending off-shelf into the Canada Basin, which are eventually converted to NO_3^- during the long residence time in Pacific waters of the Canada Basin, ultimately providing the ^{15}N-enrichment signal that characterizes Pacific UHL NO_3^-.

4.5. The origin of Pacific upper halocline layer NO_3^-

It is important to understand the origin of the nutrient maximum in the Pacific UHL in the Canada Basin (Fig. 6C) (Cooper et al., 1997; Macdonald et al. 2002; Woodgate et al., 2005; Codispoti et al., 2005), particularly NO_3^-, which, given that N* in this layer averages −10.0, is in short supply relative to the stoichiometric requirements of phytoplankton. Cooper et al. (1997) suggest that the UHL nutrient maximum is formed primarily from WW advected through Bering Strait, with only a small contribution from NH_4^+ regeneration. Similarly, we have seen that water column nitrification is likely to be very slow in summer, suggesting that regeneration may be of little importance at this time. On the other hand, there are strong build-ups of NH_4^+ that must ultimately be converted to NO_3^- in the Canada Basin (where NH_4^+ concentrations are vanishingly small). Moreover, water column nitrification is an essential step in the $\delta^{15}N_{NO_3}$ enrichment that we observe, such that regeneration must make some contribution to NO_3^- of the Pacific UHL.

Because nitrification on the Chukchi shelf contributes ^{18}O-depleted NO_3^- compared to Bering slope source waters, the $\delta^{18}O_{NO_3}$ signal reveals how much of the Pacific water NO_3^- in the Canada Basin UHL flowed through unaltered, versus being regenerated through nitrification. We calculate that 58% of the NO_3^- in the upper halocline of the Canadian Arctic was newly nitrified (Section 3.4), amounting to 7.4 of the 12.7 μM NO_3^- in the Pacific UHL. Note that this is over 3-fold higher than the 2.1 μM average NH_4^+ we observed in bottom WW of the Chukchi shelf. Cooper et al. (1997) used summer NH_4^+ concentrations to contend that regenerated N made only a small contribution (~0 to <20%) to NO_3^- in the UHL, yet our data suggest that a summertime snapshot of NH_4^+ build-ups cannot capture the total contribution of regenerated N between the Bering and Chukchi slopes, which is continuous and may be particularly important in winter, and which furnishes over half the NO_3^- in the Pacific UHL.

Our calculated contribution of 58% newly nitrified NO_3^- should be considered a minimum value, as it assumes that there are no partial NO_3^- removal processes enriching the $\delta^{18}O_{NO_3}$ signal. We do not expect partial denitrification to be an issue here, because we observed no evidence of this process on the Chukchi shelf (Section 4.4.), and because sedimentary denitrification tends to go to completion (Brandes and Devol, 1997; Lehmann et al., 2007). Phytoplankton uptake is potentially a bigger concern for this calculation, as our data show evidence of phytoplankton uptake in the southern Chukchi Sea (Figs. 4, 8 and 11). We would not expect phytoplankton uptake to be a significant problem for waters that populate the upper halocline near S~33.1, because all the waters we observed with direct evidence of phytoplankton uptake were significantly more buoyant and would have a shallower equilibrium depth in the Canada Basin. However, it is possible that upper halocline waters were affected by phytoplankton uptake in surface waters the previous year, were subsequently salinized and densified on the shelf during winter brine rejection (Cooper et al., 1997), and eventually settled in the upper halocline carrying a remnant signal of phytoplankton uptake. Kaltin and Anderson (2005) estimate that it takes on the order of one year for a water parcel to travel from the Bering slope to the Chukchi slope, which suggests that such parcels may experience both uptake and salinization from sea ice formation during their transit. If $\delta^{18}O_{NO_3}$ in the UHL is spuriously enriched by phytoplankton uptake, we would conclude that even more than 58% of the NO_3^- in the Canada Basin was regenerated.

Further insights regarding the source of NO_3^- in the Canada Basin can be gained by comparing the bottom waters of the Chukchi shelf to the basin stations (Fig. 7). The similarity of Chukchi shelf WW with the Pacific UHL in terms of both salinity and NO_3^- (Fig. 7) indicates that WW is the source of the UHL NO_3^- maximum in the Canada Basin. However, the rest of the Chukchi shelf bottom waters (non-WW) had systematically lower NO_3^- than Canada Basin waters of equal salinity (Fig. 7). This could be because these warmer waters also contain significant DON and PON that flux off-shelf and are eventually remineralized off-shelf, explaining the Canada Basin's additional NO_3^-. However, the particulate flux off of the Chukchi shelf break is thought to be low (Ashjian et al., 2005). Another possibility is that the density of WW in the Chukchi Sea varies interannually, and in other years

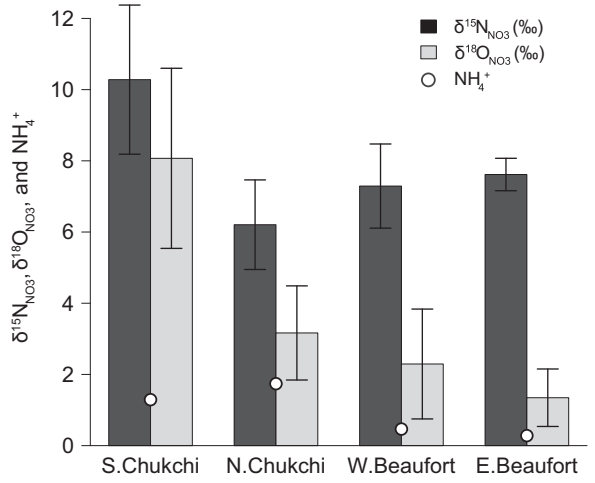

Fig. 12. $\delta^{18}O_{NO_3}$, $\delta^{15}N_{NO_3}$, and NH_4^+ concentration (white circles) in four regions of interest as delineated in Fig. 1. In the Chukchi Sea bottom waters are shown, while in the Beaufort Sea, Pacific-origin waters are shown.

one would find lighter, high NO_3^- WW that could explain the Canada Basin NO_3^- signal. Clearly, year-round measurements of nutrient concentrations on the Chukchi shelf are crucial to understand the seasonal dynamics and the origin of Canada Basin NO_3^-.

4.6. *Using stable isotopes to trace the flow of Pacific waters*

The stable isotopic signature of NO_3^- in the Chukchi shelf and Canada Basin point to two main processes: (1) phytoplankton uptake, imparting a ~1:1 slope in $\delta^{18}O_{NO_3}$ versus $\delta^{15}N_{NO_3}$ (the "uptake line", Fig. 11), and (2) CPND, imparting a negative slope (the "remineralization line"). These uptake and remineralization lines reflect the flow of Pacific waters across the Chukchi Sea and into the Canada Basin, as traced out in Fig. 11. The flow begins in the upper right with Bering Strait waters that are severely affected by phytoplankton uptake, then proceeds towards the lower left, where waters with successively less phytoplankton uptake flowed through Bering Strait at an earlier stage in the growth season. We then encounter WW on the Chukchi shelf, which harbors no direct phytoplankton uptake signal, and is very close to the original Bering slope source waters ($\delta^{15}N_{NO_3}$ ~6.5 and $\delta^{18}O_{NO_3}$ ~3.2; Table 1), albeit with a small signal of water column nitrification. Turning the corner towards the lower right, following the "remineralization line", are waters that populate the Pacific UHL, whose NO_3^- has been ^{15}N-enriched and ^{18}O-depleted relative to source waters, due to the process of CPND.

The isotopic signature of Pacific-origin waters propagates far northward into the Canada Basin, as well as a great distance eastward along the continued pathway (the Beaufort shelfbreak jet; Nikolopoulos et al., 2009) towards the Canadian Arctic Archipelago and Fram Strait (Fig. 12). We observed this signature as far east as the Amundsen Gulf, the first entrance of Pacific waters to the Archipelago. Examining the phytoplankton bloom of the North Water Polynya, Tremblay et al. (2006) use PON to estimate that initial $\delta^{15}N_{NO_3}$ was 8.4‰, similar to our values in the UHL of the Canada Basin. Therefore, it is likely that the $^{15}N_{NO_3}$ enrichment signature of the Chukchi shelf pervades the entire western Arctic, a tracer of Pacific-origin water that is isolated from mixing of heavier Atlantic water by the strong stratification of the halocline.

Granger et al. (2011) hypothesize that this Pacific water isotopic signature is conferred primarily from CPND taking place on the Bering Sea eastern shelf. However, this is inconsistent with observations that the input of N to the Arctic occurs almost exclusively through the Anadyr water that upwells on the northern Bering shelf and flows through western Bering Strait into the Chukchi Sea. It is these Anadyr waters, not the transformed waters from the Eastern Bering shelf, that supply 95% of NO_3^- to the Chukchi Sea and downstream Arctic Ocean (Walsh et al., 1989). This is consistent with the results of Cooper et al. (1997), who used nutrient, salinity, and $\delta^{18}O_{H_2O}$ tracers to show that the UHL of the Canada Basin is fed by waters originating in the Gulf of Anadyr. It is also consistent with our nutrient results and those of Hansell et al. (1993), showing a complete lack of NO_3^- in warm ACC waters along the Alaskan coast (Fig. 4A and B), which are fed from the Eastern Bering Sea. Therefore, because CPND occurs independently on the Chukchi shelf, we argue that it is the north Bering and Chukchi seas in the flow path of Anadyr waters that primarily generate the ^{15}N enrichment that characterizes the NO_3^- of the Pacific Arctic Ocean.

In the deeper Atlantic layer, the NO_3^- isotopic signature is similar to deep water values that have been measured throughout the global ocean (Sigman et al., 2009). It is interesting to note that Pacific source waters from the Bering slope are isotopically similar to these deep Atlantic waters, but ~1‰ heavier in $\delta^{15}N_{NO_3}$, perhaps a residual signal of partial water column denitrification or CPND in the long meridional overturning circulation pathway to the North Pacific.

5. Conclusion

Between the Bering and Chukchi slopes, NO_3^- drops from ~20 to 12.7 μm, a net loss of ~7 μM NO_3^- (Table 1). We have argued that this loss should not be thought of as a direct flux of NO_3^- from the water column into sediments that is lost to denitrification. Instead, this NO_3^- loss is driven primarily by phytoplankton uptake in the upper water column of the Chukchi Sea. As these waters transit the broad shelf, cooling and brine rejection during ice formation may mix the water column completely. This combines waters affected by uptake with those that are not, creating dense WW of intermediate nutrient content (Cooper et al., 1997), which ultimately populate the Pacific UHL. Meanwhile, summer waters fluxing through well-mixed Bering Strait are stripped of nutrients throughout the entire water column, and ultimately find an equilibrium depth above the Pacific UHL (50–80 m), contributing to the perennially low nutrient concentrations in the strongly-stratified upper Canada Basin.

Much of the organic N produced by phytoplankton on the Chukchi shelf reaches the sediments, where it may be lost permanently through either burial or partial nitrification coupled to denitrification (Henriksen et al., 1993; Granger et al., 2011; Horak et al., 2013). The remainder of this organic N is returned to the water column above as NH_4^+, where its eventual nitrification supplies at least 58% of the 12.7 μM NO_3^- in the Pacific UHL, and imparts ^{15}N enrichment and ^{18}O depletion to Pacific NO_3^-. This isotopic signature pervades the Pacific layer and propagates eastward, reaching at least as far the Canadian Arctic Archipelago.

At the time of our sampling, rates of O_2 consumption suggest that remineralization and nitrification occurred primarily in the sediments. Nevertheless, water column nitrification is an essential step in the ^{15}N enrichment we observed—this water column nitrification may largely happen in the winter and/or once waters have been fluxed off the shelf, separating them from the continual shelf sediment source of NH_4^+.

DIN concentrations in the Canada Basin are generally much higher than on the shelf for any given density, suggesting that shelf DIN must be higher in winter than when we sampled in summer. In addition, although we suggest that water column nitrification slows in summer, causing summertime accumulations of NH_4^+ on the Chukchi shelf, these seasonal dynamics remain uncertain. For both of these reasons, an annual time series of NO_3^-,

NO_2^-, and NH_4^+ would be extremely useful for understanding the seasonal dynamics of the N-cycle on the Chukchi shelf.

Acknowledgements

This work was supported by NASA grant NNX10AF42G to K. Arrigo, R. Pickart, and J. Swift, and NASA grant NNX11AL52H to Z. Brown. We thank Lee Cooper for providing $\delta^{18}O_{H_2O}$ data. We are grateful to the captain and crew of the USCGC *Healy* for their hard work and assistance.

References

Aagaard, K., Coachman, L.K., Carmack, E., 1981. On the halocline of the Arctic Ocean. Deep Sea Res. Part A: Oceanogr. Res. Pap. 28, 529–545.
Arrigo, K.R., van Dijken, G.L., 2011. Secular trends in Arctic Ocean net primary production. J. Geophys. Res. 116, C09011.
Arrigo, K.R., Perovich, D.K., Pickart, R.S., Brown, Z.W., van Dijken, G.L., Lowry, K.E., Mills, M.M., Palmer, M.A., Balch, W.M., Bahr, F., Bates, N.R., Benitez-Nelson, C., Bowler, B., Brownlee, E., Ehn, J.K., Frey, K.E., Garley, R., Laney, S.R., Lubelczyk, L., Mathis, J., Matsuoka, A., Mitchell, B.G., Moore, G.W.K., Ortega-Retuerta, E., Pal, S., Polashenski, C.M., Reynolds, R.A., Schieber, B., Sosik, H.M., Stephens, M., Swift, J.H., 2012. Massive phytoplankton blooms under Arctic Sea Ice. Science 336, 1408.
Armstrong, F.A.J., Stearns, C.R., Strickland, J.D.H., 1967. The measurement of upwelling and subsequent biological processes by means of the Technicon Autoanalyzer and associated equipment. Deep-Sea Res. 14, 381–389.
Ashjian, C.J., Gallager, S.M., Plourde, S., 2005. Transport of plankton and particles between the Chukchi and Beaufort Seas during summer 2002, described using a Video Plankton Recorder. Deep-Sea Res. Part II 52, 3259–3280.
Avak, H., Fry, B., 1999. EA-IRMS: Precise and Accurate Measurement of $\delta^{15}N$ on <10 μg N, Finnigan MAT Appl. Flash Rep. G29, Thermoquest, Egelsbach, Germany.
Bernhardt, H., Wilhelms, A., 1967. The continuous determination of low level iron, soluble phosphate and total phosphate with the AutoAnalyzer. Tech. Symp. I, 385–389.
Böhlke, J.K., Mroczkowski, S.J., Coplen, T.B., 2003. Oxygen isotopes in nitrate: new reference materials for ^{18}O:^{17}O:^{16}O measurements and observations on nitrate–water equilibration. Rapid Commun. Mass Spectrom. 17, 1835–1846.
Brandes, J.A., Devol, A.H., 1997. Isotoopic fractionation of oxygen and nitrogen in coastal marine sediments. Geochim. Cosmochim. Acta 61, 1793–1801.
Brown, Z.W., Arrigo, K.R., 2012. Contrasting trends in sea ice and primary production in the Bering Sea and Arctic Ocean. ICES J. Mar. Sci. 69, 1180–1193.
Buchwald, C., Santoro, A.E., McIlvin, M.R., Casciotti, K.L., 2012. Oxygen isotopic composition of nitrate and nitrite produced by nitrifying cocultures and natural marine assemblages. Limnol. Oceanogr. 57, 1361.
Casciotti, K.L., Sigman, D.M., Hastings, M.G., Böhlke, J.K., Hilkert, A., 2002. Measurement of the oxygen isotopic composition of nitrate in seawater and freshwater using the denitrifier method. Anal. Chem. 74, 4905–4912.
Chang, B.X., Devol, A.H., 2009. Seasonal and spatial patterns of sedimentary denitrification rates in the Chukchi Sea. Deep Sea Res. Part II 56, 1339–1350.
Christman, G.D., Cottrell, M.T., Popp, B.N., Gier, E., Kirchman, D.L., 2011. Abundance, diversity, and activity of ammonia-oxidizing prokaryotes in the coastal Arctic Ocean in summer and winter. Appl. Environ. Microbiol. 77, 2026–2034.
Cooper, L.W., Whitledge, T.E., Grebmeier, J.M., Weingartner, T., 1997. The nutrient, salinity, and stable oxygen isotope composition of Bering and Chukchi Seas waters in and near the Bering Strait. J. Geophys. Res. 102, 12563–12573.
Cooper, L.W., Sexson, M.G., Grebmeier, J.M., Grandinger, R., Mordy, C.W., Lovvorn, J.R., 2013. Linkages between sea ice coverage, pelagic-benthic coupling and the distribution of spectacled eiders: observations in March 2008, 2009 and 2010 from the Northern Bering Sea. Deep-sea Res. Part II , http://dx.doi.org/10.1016/j.dsr2.2013.03.009.
Codispoti, L.A., Friederich, G.E., Sakamoto, C.M., Gordon, L.I., 1991. Nutrient cycling and primary production in the marine systems of the Arctic and Antarctic. J. Mar. Syst. 2, 359–384.
Codispoti, L.A., Flagg, C., Kelly, V., Swift, J.H., 2005. Hydrographic conditions during the 2002 SBI process experiments. Deep Sea Res. Part II 52, 3199–3226.
Codispoti, L.A., Flagg, C.N., Swift, J.H., 2009. Hydrographic conditions during the 2004 SBI process experiments. Deep Sea Res. Part II 56, 1144–1163.
Deal, C.J., Meibing, J., Jia, W., 2008. The significance of water column nitrification in the southeastern Bering Sea. Chin. J. Polar Sci. 19, 185–192.
Degobbis, D., 1973. On the storage of seawater samples for ammonia determination. Limnol. Oceanogr. 18, 146–150.
Deutsch, C., Weber, T., 2012. Nutrient ratios as a tracer and driver of ocean biogeochemistry. Annu. Rev. Mar. Sci. 4, 113–141.
Devol, A.H., Codispoti, L.A., Christensen, J.P., 1997. Summer and winter denitrification rates in western Arctic shelf sediments. Cont. Shelf Res. 17, 1029–1050.
Granger, J., Sigman, D.M., Needoba, J.A., Harrison, P.J., 2004. Coupled nitrogen and oxygen isotope fractionation of nitrate during assimilation by cultures of marine phytoplankton. Limnol. Oceanogr. 49, 1762–1773.
Granger, J., Prokopenko, M.G., Sigman, D.M., Mordy, C.W., Morse, Z.M., Morales, L.V., Sambrotto, B., Plessen, B., 2011. Coupled nitrification-denitrification in sediment of the eastern Bering shelf leads to ^{15}N enrichment of fixed N in shelf waters. J. Geophys. Res. 116, C11006.
Granger, J., Prokopenko, M.G., Mordy, C.W., Sigman, D.M., 2013. The proportion of remineralized nitrate on the ice-covered eastern Bering Sea shelf evidenced from the oxygen isotope ratio of nitrate. Global Biogeochem. Cycles 27, 1–10.
Grebmeier, J.M., McRoy, C.P., 1989. Pelagic-benthic coupling on the shelf of the northern Bering and Chukchi Seas. III. Benthic food supply and carbon cycling. Mar. Ecol. Prog. Ser. 53, 79–91.
Gruber, N., Sarmiento, J., 1997. Global patterns of marine nitrogen fixation and denitrification. Global Biogeochem. Cycles 11, 235–266.
Hansell, D.A., Whitledge, T.E., Goering, J.J., 1993. Patterns of nitrate utilization and new production over the Bering–Chukchi shelf. Cont. Shelf Res. 13, 601–627.
Hansell, D.A., Kadko, D., Bates, N.R., 2004. Degradation of terrigenous dissolved organic carbon in the western Arctic Ocean. Science 304, 858–861.
Henriksen, K., Blackburn, T.H., Lomstein, B.A., McRoy, C.P., 1993. Rates of nitrification, distribution of nitrifying bacteria and inorganic N fluxes in northern Bering–Chukchi shelf sediments. Cont. Shelf Res. 13, 629–651.
Henriksen, K., Kemp, W.M., 1988. Nitrification in estuarine and coastal marine sediments. In: Blackburn, T.H., Sørensen, J. (Eds.), Nitrogen Cycling in Coastal Marine Environments. John Wiley & Sons, Chichester, pp. 207–249.
Hirota, A., Ijiri, A., Komatsu, D.D., Ohkubo, S.B., Nakagawa, F., Tsunogai, U., 2009. Enrichment of nitrous oxide in the water columns in the area of the Bering and Chukchi Seas. Mar. Chem. 116, 47–53.
Horak, R.E.A., Whitney, H., Shull, D.H., Mordy, C.W., Devol, A.H., 2013. The role of sediments on the Bering shelf N cycle: insights from measurements of benthic denitrification and benthic DIN fluxes. Deep-Sea Res. Part II , http://dx.doi.org/10.1016/j.dsr2.2013.03.014.
Kaltin, S., Anderson, L.G., 2005. Uptake of atmospheric carbon dioxide in Arctic shelf seas: evaluation of the relative imporance of processes that influence pCO_2 in water transported over the Bering–Chukchi shelf. Mar. Chem. 94, 67–79.
Karsh, K.L., Granger, J., Kritee, K., Sigman, D.M., 2012. Eukaryotic assimilatory nitrate reductase fractionates N and O isotopes with a ratio near unity. Environ. Sci. Technol. 46, 5727–5735.
Kerouel, R., Aminot, A., 1997. Fluorometric determination of ammonia in sea and estuarine waters by direct segmented flow analysis. Mar. Chem. 57, 265–275.
Lehmann, M.F., Sigman, D.M., McCorkle, D.C., Granger, J., Hoffmann, S., Cane, G., Brunelle, B.G., 2007. The distribution of nitrate $^{15}N/^{14}N$ in marine sediments and the impact of benthic nitrogen loss on the isotopic composition of oceanic nitrate. Geochim. Cosmochim. Acta 71, 5384–5404.
Loeng, H., Brander, K., Carmack, E., Denisenko, S., Drinkwater, K., Hansen, B., Kovacs, K., Livingston, P., McLaughlin, F., Sakshaug, E., 2005. Marine systems, Arctic Climate Impact Assessment. Cambridge University Press, Cambridge, pp. 454–524.
Lomstein, B.A., Blackburn, T.H., Henriksen, K., 1989. Aspects of nitrogen and carbon cycling in the northern Bering Shelf sediment. I. The significance of urea turnover in the mineralization of NH_4^+. Mar. Ecol. Prog. Ser. 57, 237–247.
Macdonald, R.W., McLaughlin, F.A., Carmack, E.C., 2002. Fresh water and its sources during the SHEBA drift in the Canada Basin of the Arctic Ocean. Deep Sea Res. Part I 49, 1769–1785.
Mordy, C.W., Cokelet, E.D., Ladd, C., Menzia, F.A., Proctor, P., Stabeno, P.J., Wisegarver, E., 2012. Net community production on the middle shelf of the eastern Bering Sea. Deep Sea Res. Part II 65-70, 110–125.
Nikolopoulos, A., Pickart, R.S., Fratantoni, P.S., Shimada, K., Torres, D.J., Jones, E.P., 2009. The western Arctic boundary current at 152°W: structure, variability, and transport. Deep Sea Res. Part II 56, 1164–1181.
Padman, L., Erofeeva, S., 2004. A barotropic inverse tidal model for the Arctic Ocean. Geophys. Res. Lett. 31 (2), L02303.
R Development Core Team, 2011. R: A Language and Environment for Statistical Computing. R Foundation for Statistical Computing, Vienna, Austria. ⟨http://www.R-project.org/⟩.
Rowe, G.T., Phoel, W.C., 1992. Nutrient regeneration and oxygen demand in Bering Sea continental shelf sediments. Cont. Shelf Res. 12, 439–449.
Rysgaard, S., Thamdrup, B., Risgaard-Petersen, N., Fossing, H., Berg, P., Christensen, P.B., Dalsgaard, T., 1998. Seasonal carbon and nutrient mineralization in a high-Arctic coastal marine sediment, Young Sound, Northeast Greenland. Mar. Ecol. Prog. Ser. 175, 261–276.
Sakshaug, E., 2004. Primary and secondary production in the Arctic Seas. In: Steain, R., Macdonald, R.W. (Eds.), The Organic Carbon Cycle in the Arctic Ocean. Springer, Berlin Heidelberg New York, pp. 57–81.
Sarmiento, J.L., Gruber, N., 2006. Ocean Biogeochemical Dynamics. Princeton University Press, Princeton p. 503.
Sigman, D.M., Casciotti, K.L., Andreani, M., Barford, C., Galanter, M., Böhlke, J.K., 2001. A bacterial method for the nitrogen isotopic analysis of nitrate in seawater and freshwater. Anal. Chem. 73, 4145–4153.
Sigman, D.M., DiFiore, P.J., Hain, M.P., Deutsch, C., Karl, D.M., 2009. Sinking organic matter spreads the nitrogen isotope signal of pelagic denitrification in the North Pacific. Geophys. Res. Lett. 36, L08605.
Simpson, K.G., Tremblay, J.E., Gratton, Y., Price, N.M., 2008. An annual study of inorganic and organic nitrogen and phosphorus and silicic acid in the southeastern Beaufort Sea. J. Geophys. Res. 113, C07016.
Spall, M.A., Pickart, R.S., Fratantoni, P.S., Plueddemann, A.J., 2008. Western Arctic shelfbreak eddies: formation and transport. J. Phys. Oceanogr. 38, 1644–1668.
Tremblay, J.E., Michel, C., Hobson, K.A., Gosselin, M., Price, N.M., 2006. Bloom dynamics in early opening waters of the Arctic Ocean. Limnol. Oceanogr. 51, 900–912.

Tanaka, T., Guo, Laodong, Deal, C., Tanaka, N., Whitledge, T., Murata, A., 2004. N deficiency in a well-oxygenated cold bottom water over the Bering shelf: influence of sedimentary denitrification. Cont. Shelf Res. 24, 1271–1283.
Walsh, J.J., McRoy, C.P., Coachman, L.K., Goering, J.J., Nihoul, J.J., Whitledge, T.E., Blackburn, T.H., Parker, P.L., Wirick, C.D., Shuert, P.G., Grebmeier, J.M., Springer, A.M., Tripp, R.D., Hansell, D.A., Djenidi, S., Deleersnijder, E., Henriksen, K., Lund, B.A., Andersen, P., Müller-Karger, F.E., Dean, K., 1989. Carbon and nitrogen cycling within the Bering/Chukchi Seas: source regions for organic matter effecting AOU demands of the Arctic Ocean. Prog. Oceanogr., 22; , pp. 277–359.
Whitledge, T.E., Reeburgh, W.S., Walsh, J.J., 1986. Seasonal inorganic nitrogen distributions and dynamics in the southeastern Bering Sea. Cont. Shelf Res. 5, 109–132.
Woodgate, R.A., Aagaard, K., Weingartner, T.J., 2005. A year in the physical oceanography of the Chukchi Sea: moored measurements from autumn 1990–1991. Deep-Sea Res. Part II 52, 3116–3149.
Woodgate, R.A., Weingartner, T.J., Lindsay, R., 2012. Observed increases in Bering Strait oceanic fluxes from the Pacific to the Arctic from 2001 to 2011 and their impacts on the Arctic Ocean water column. Geophys. Res. Lett. 39, L24603.
Yamamoto-Kawai, M., Carmack, E., McLaughlin, F., 2006. Nitrogen balance and Arctic throughflow. Nature 443, 43.